EXAFS- a local structural probe for material characterization

K. R. Priolkar

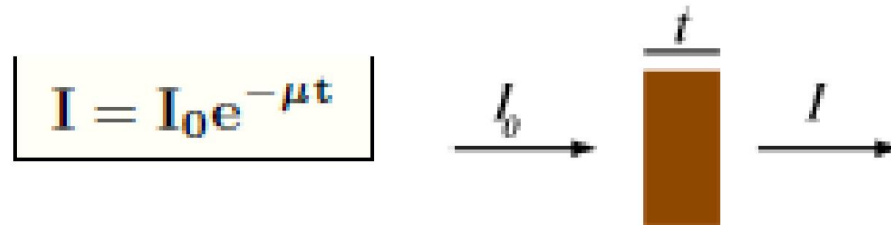Department of Physics

Goa University, Goa 403 206 India

Plan

- History
- EXAFS
  - Fundamentals
  - Experiment
  - Data Analysis
- XANES
- Examples
  - FSMA – Ni_2MnGa
  - Multiferroic – $YMnO_3$
  - Magnetocaloric – Gd_5Ge_4
  - Cobaltites
  - Others….

X-ray Absorption Coefficient

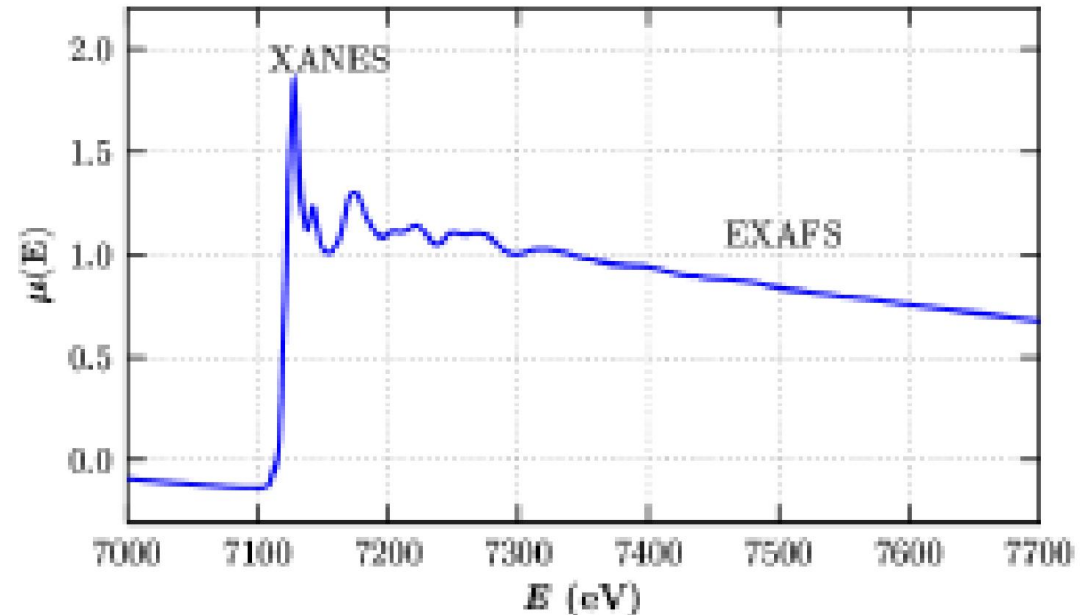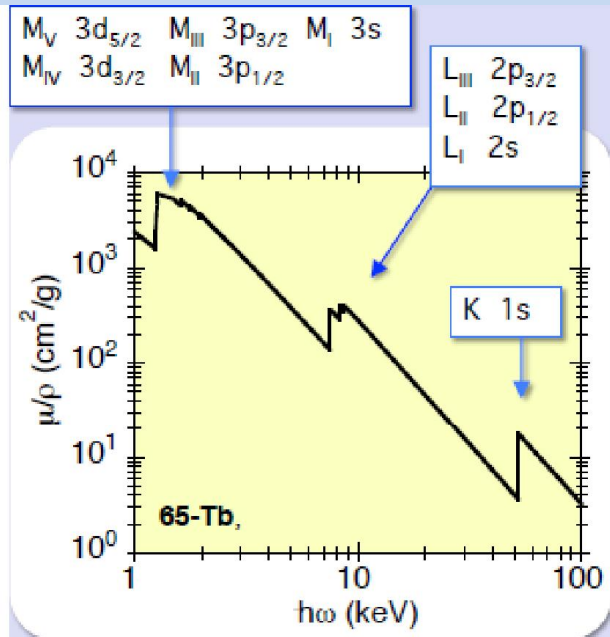The intensity of an x-ray beam passing through a material of thickness *t* is given by the absorption coefficient *μ*:

$$I = I_0 e^{-\mu t}$$

I_0 – incident x-ray intensity
I – transmitted x-ray intensity

μ depends strongly on energy of X-rays, *E* and atomic number *Z*.

$$\mu \approx \frac{\rho Z^4}{A E^3}$$

Definition

X-ray absorption fine structure (**XAFS**) is the modulation of the x-ray absorption coefficient near or above an absorption edge. XAFS is also referred to as X-ray Absorption Spectroscopy (**XAS**) and is divided in two regimes:

XANES – X-ray Absorption Near Edge Structure
EXAFS – Extended X-ray Absorption Fine Structure

History

- X-ray Absorption Edges were discovered in 1912
- X-ray absorption fine structure (XAFS) spectroscopy was first noticed in 1920's [Near Edge structure in 1920 and Extended structure in 1929].
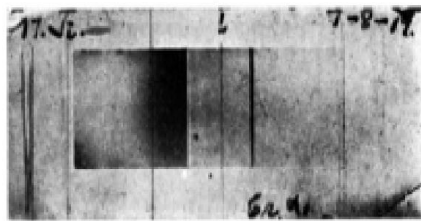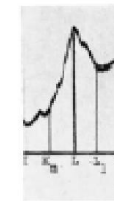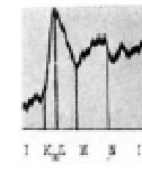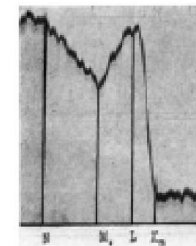

Fig. 1. Aluminium.
Fig. 2. Phosphorus.
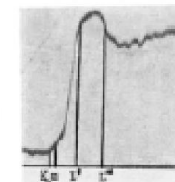Fig. 3. Sulphur.
Fig. 4. Potassium.
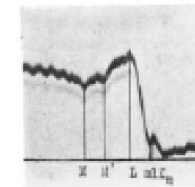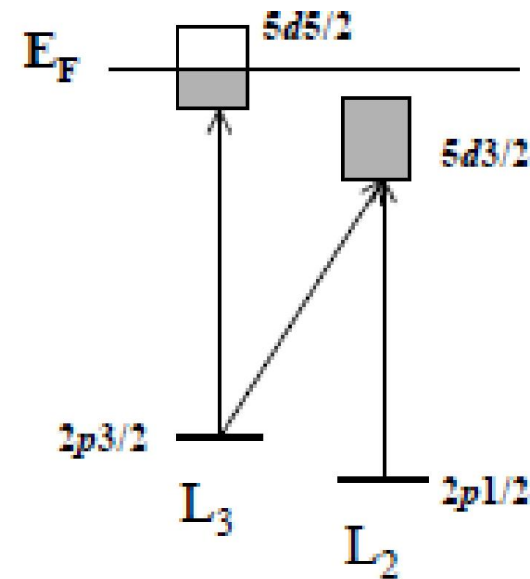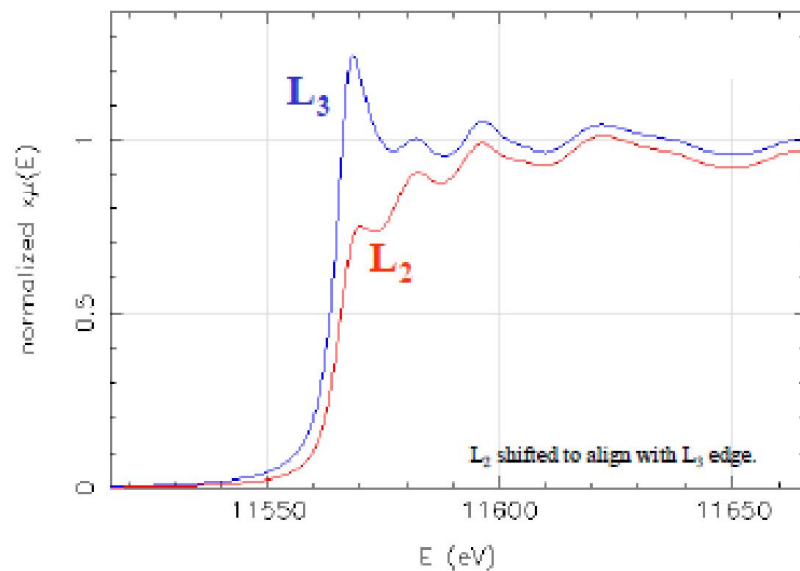Fig. 5. Scandium.
Fig. 6. Titanium.
Fig. 7. Vanadium.
Fig. 8. Chromium.

Phys. Rev. 16, 202 (1920)

- At that time spectroscopy was explained by electronic energy levels of Bohr. Near Edge fit Bohr, but not Extended.

- Kronig in 1931, 1932 in 2 publications proposed EXAFS LRO theory based on electron energy bands and gaps in solids (Bloch).

- After discovery that XAFS occurred in molecules Kronig in 1934 proposed a completely different theory, SRO theory, (related to modern theory except did not include Debye-Waller factor, mean free path and the correct phase shift. Also could not calculate the photoelectron-atom interaction correctly-no computers!)

- **EXAFS first called Kronig Structure.** Kronig never appreciated that SRO correct for both molecules and solids, and LRO theory wrong, causing confusion for 40 years.

  Disagreement between theory and experiment because both were wrong!

Extended Fine Structure in X-Ray Absorption Spectra of Certain Perovskites

Joseph Perel*

and

Richard D. Deslattes

National Bureau of Standards, Washington, D. C. 20234
(Received 9 July 1969)

In this paper we attempt to test the validity of the short-range-order (SRO) and the long-range-order (LRO) theories of the extended fine structure (EFS) in x-ray absorption spectra. This is done by comparing the EFS's of Ti, Ca, Zr, and Sr in the perovskitelike compounds $SrTiO_3$, $CaTiO_3$, $SrZrO_3$, and $CaZrO_3$. The regularities which have been anticipated from SRO or LRO theories have not been observed. We are thus led to suggest that models are required other than those which have been used to explain the EFS.

- In 1965 E. A. Stern joined hands with Farrel Lytle at University of Washington. Lytle had a lab facility measuring EXAFS (before hard x-ray Synchrotron Radiation sources).

- Dale Sayers, a grad student at UW, joined the duo to work for his Ph.D. thesis on EXAFS: develop theory with Stern and measure with Lytle.

- Their work showed the mistake in Kronig LRO; gave standard and general form for XAFS in SS; shows that the photoelectron-atom parameters are transferable between known structures and thus can be used to determine unknown ones for SS.

New Technique for Investigating Noncrystalline Structures: Fourier Analysis of the Extended X-Ray—Absorption Fine Structure*

Dale E. Sayers† and Edward A. Stern†‡

Department of Physics, University of Washington, Seattle, Washington 98105

and

Farrel W. Lytle

Boeing Scientific Research Laboratories, Seattle, Washington 98124
(Received 16 July 1971)

We have applied Fourier analysis to our point-scattering theory of x-ray absorption fine structure to invert experimental data formally into a radial structure function with determinable structural parameters of distance from the absorbing atom, number of atoms, and widths of coordination shells. The technique is illustrated with a comparison of evaporated and crystalline Ge. We find that the first and second neighbors in amorphous Ge are at the crystalline distance within the accuracy of measurement (1%).

[Theory of the extended x-ray-absorption fine structure](#) Edward A. Stern

[Extended x-ray-absorption fine-structure technique. II. Experimental practice and selected results](#) F. W. Lytle, D. E. Sayers, and E. A. Stern

[Extended x-ray-absorption fine-structure technique. III. Determination of physical parameters](#) E. A. Stern, D. E. Sayers, and F. W. Lytle

XAFS – Modern Theory

- **X-ray Absorption Fine Structure (XAFS)** is ideally suited to map such local distortions in structure.
  - It results from interference of outgoing and back scattered photoelectron waves.
  - The range of photoelectron is limited due to core-hole life time.
  - Photoelectron can also be scattered inelastically.

X-ray Absorption Fine Structure (XAFS)

- Modulation of X-ray intensities near or above an X-ray absorption edge.

- Broadly divided in two regions
  - XANES – X-ray Absorption Near Edge Structure
  - EXAFS – Extended X-ray Absorption Fine Structure

- Contain related but slightly different information about an element's local coordination and chemical state.

- It applies to any element, works at low concentrations and minimal sample requirements.
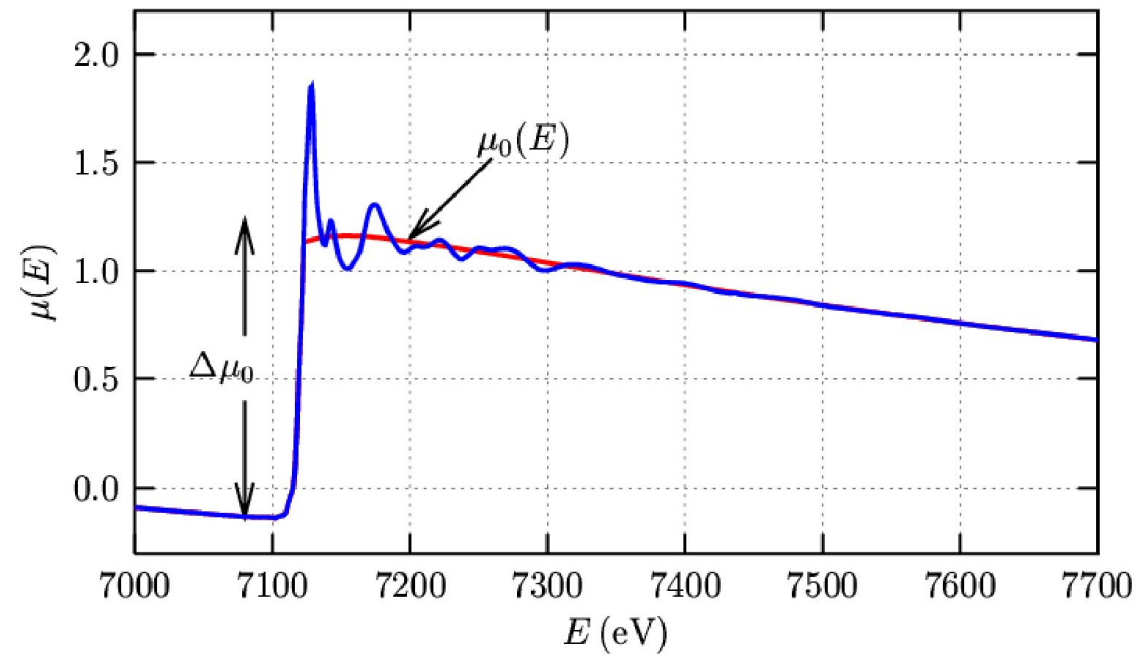
$I = I_0 \exp(-\mu t)$ or $\mu(E) = \ln(I_0/I)$

$$\chi(E) = \frac{\mu(E) - \mu_0(E)}{\Delta\mu_0(E_0)}$$

XAFS: Fundamentals
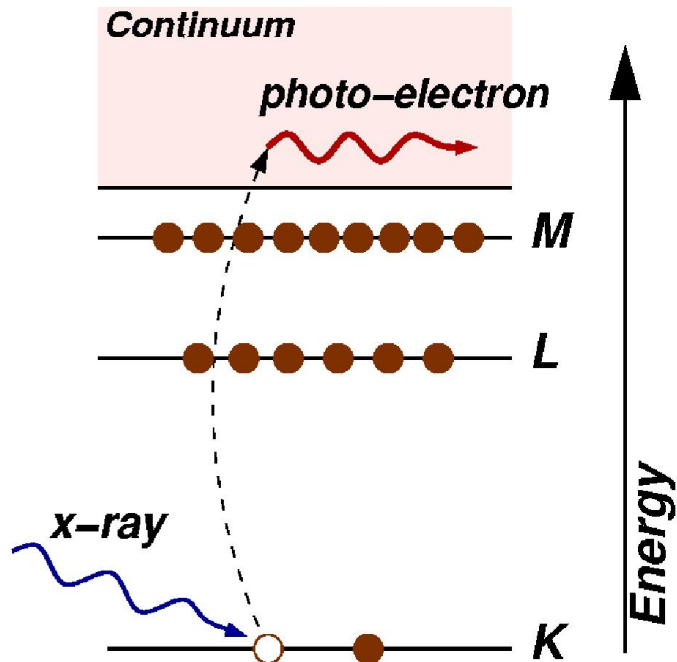
The amplitude of the back scattered photo-electron at the absorbing atom will vary with energy causing oscillations in $\mu(E)$ that are the XAFS.
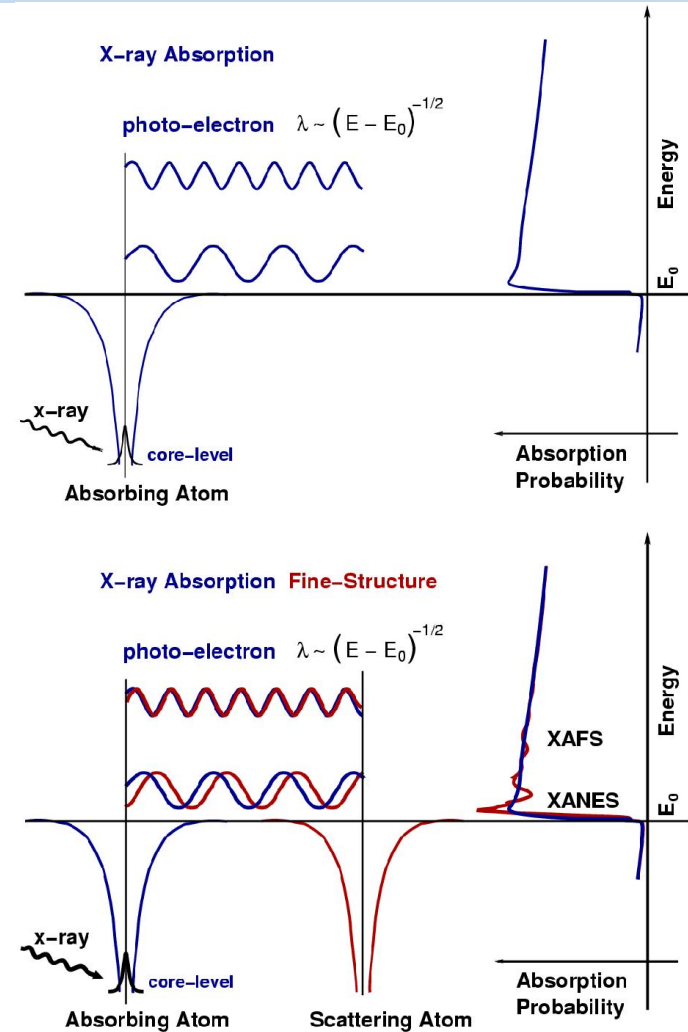
EXAFS Equation

The initial state **|i>** - x-ray photon + core level electron

The final state **|f>** - core hole + photoelectron in the continuum

Fermi's Golden Rule describes $\mu(E)$ as a transition between quantum states:

$$\mu(E) \sim |\langle i|\mathcal{H}|f\rangle|^2$$

$\langle i|$ the *initial state* describes the core level (and the photon). This is not altered by the neighboring atom.

$\mathcal{H}$ the *interaction*. In the dipole approximation, $\mathcal{H} = e^{ikr} \approx 1$.

$|f\rangle$ the *final state* describes the photo-electron (and no photon). This is altered by the neighboring atom.

We are interested in the transition rate between core level (e.g. 1s) and final states that is induced by a weak time-dependent perturbation such as x-ray photon.

The interaction Hamiltonian (to first order in field) $\mathcal{H} \propto \vec{A} \cdot \vec{p}$,
$\vec{A}$ - vector potential and $\vec{p}$ - momentum operator of electron

Using commutation relations with the Hamiltonian,

$$\mu \propto |< f|\hat{\epsilon} \cdot \vec{r} e^{i\vec{k}\cdot\vec{r}}|i >|^2 \qquad \vec{k} \cdot \vec{r} \ll 1$$

In dipole approximation

$$\mu \propto |< f|\hat{\epsilon} \cdot \vec{r}|i >|^2$$

$$k = \frac{2\pi}{\lambda}$$

$$\lambda \approx \frac{1}{Z^2} \qquad r \approx \frac{a_0}{Z}$$

Writing $|f\rangle = |f_0 + \Delta f\rangle$, where Δf gives the change in photo-electron final state due to backscattering from the neighboring atom, we can expand μ to get

$$\mu(E) \sim |\langle i|\mathcal{H}|f_0\rangle|^2 \left[1 + \frac{\langle i|\mathcal{H}|\Delta f\rangle \langle f_0|\mathcal{H}|i\rangle^*}{|\langle i|\mathcal{H}|f_0\rangle|^2} + C.C \right]$$

Comparing this to our definition for χ,

$$\mu(E) = \mu_0(E)[1 + \chi(E)],$$

and recognizing that $\mu_0(E)$ is given by $|\langle i|\mathcal{H}|f_0\rangle|^2$, we see that

$$\chi(E) \sim \langle i|\mathcal{H}|\Delta f\rangle \sim \langle i|\Delta f\rangle.$$

Since the *initial state* for the core-level is very nearly a delta-function in space (centered at the absorbing atom), this becomes

$$\chi(E) \approx \int dr \delta(r) \psi_{\text{scatt}}(r) = \psi_{\text{scatt}}(0).$$

XAFS is due to oscillations in the photoelectron wave-function at the absorbing atom caused by its scattering by neighbouring atoms.

With $\chi \sim \psi_{\text{scatt}}(0)$, we can build a simple model for χ from the photo-electron:

1. leaving the absorbing atom

2. scattering from the neighbor atom

3. returning to the absorbing atom
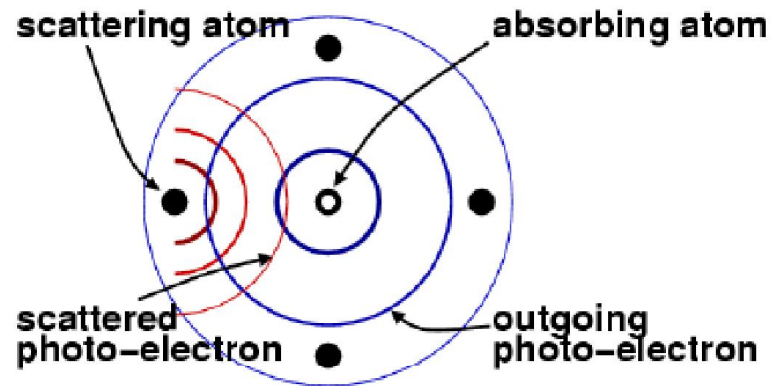
$$\chi(k) = \frac{e^{ikR}}{kR} \left[2kf(k)e^{i\delta(k)} \right] \frac{e^{ikR}}{kR} + C.C.$$

$$\chi(k) = \frac{f(k)}{kR^2} \sin[2kR + \delta(k)]$$

$$\chi(k) = \frac{Nf(k)e^{-2k^2\sigma^2}}{kR^2} \sin[2kR + \delta(k)]$$

Central atom

Backscattering atom
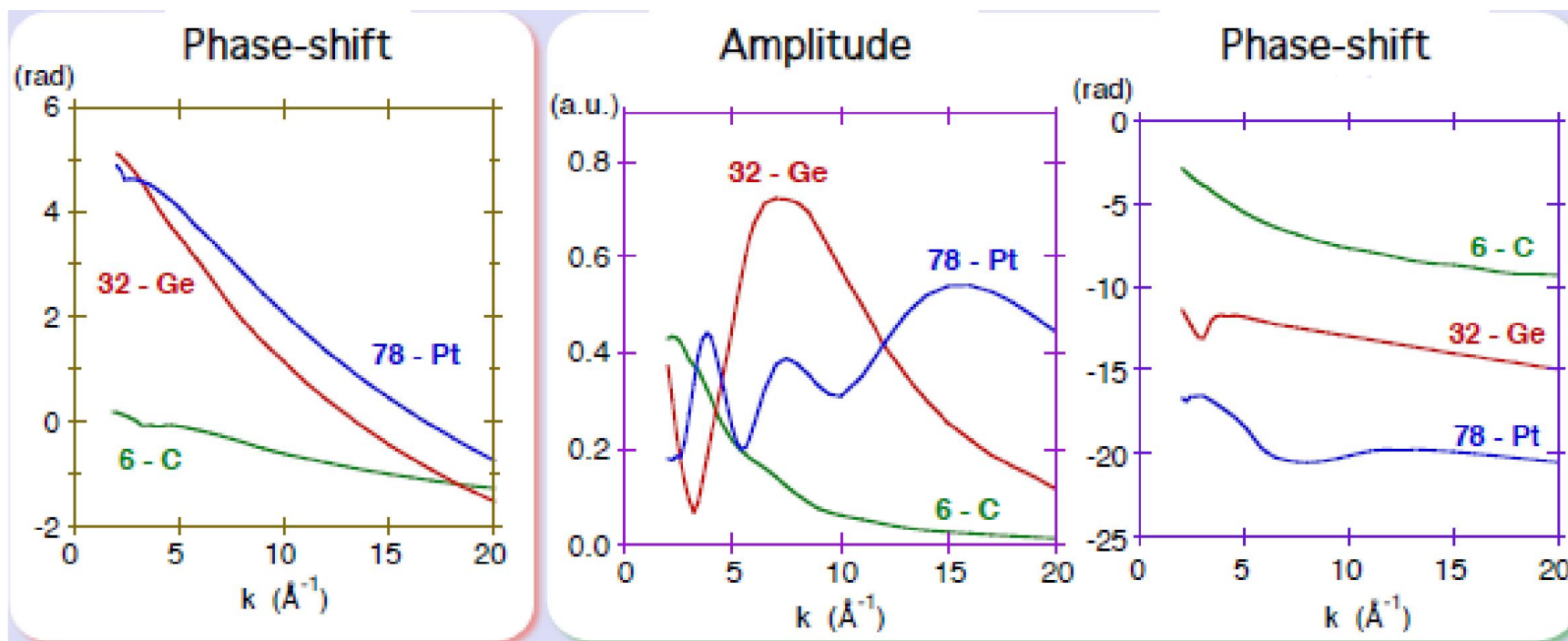
Calculated by FEFF 6.01

Z dependence

Sensitivity to atomic species
$(Z - Z') \geq 5$

Thermal disorder

Period of atomic vibrations
$$\tau_{vib} \approx 10^{-12}\ s$$

A   B
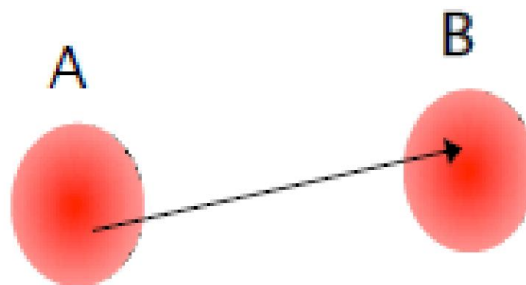
Photoelectron time of flight
$$\tau_{EXAFS} \approx 10^{-15}\ s$$

One photoelectron $\longrightarrow$ Instantaneous distance

EXAFS Spectrum $\longrightarrow$ Distribution of distances

EXAFS formula
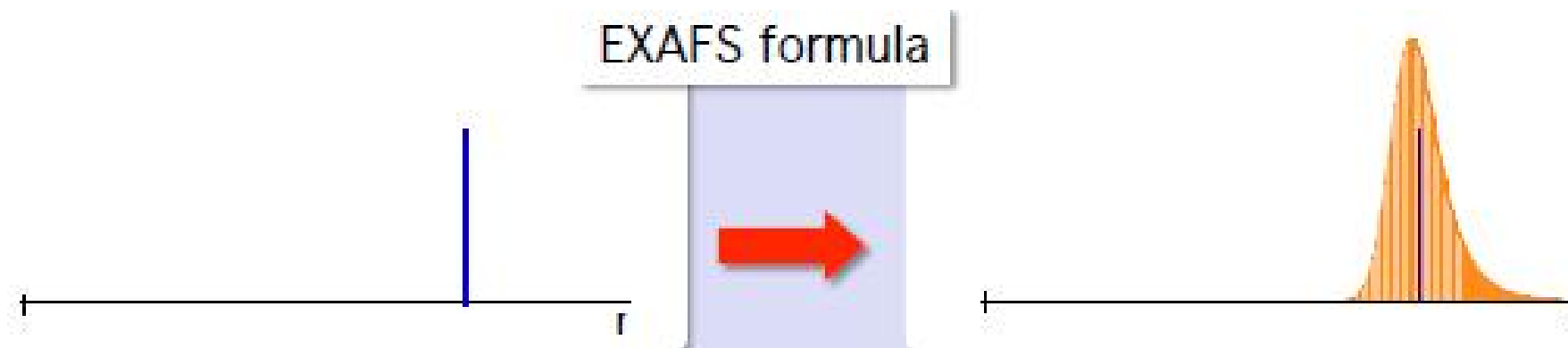
Structural disorder

Distorted shells in crystals
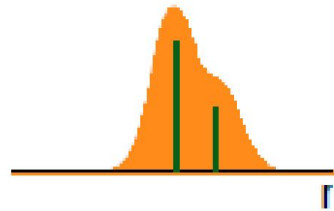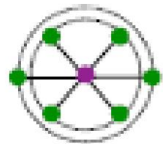
Sites disorder in crystals
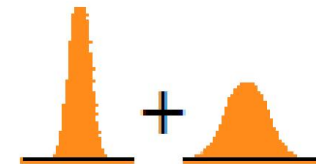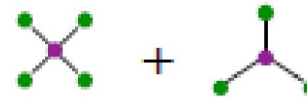
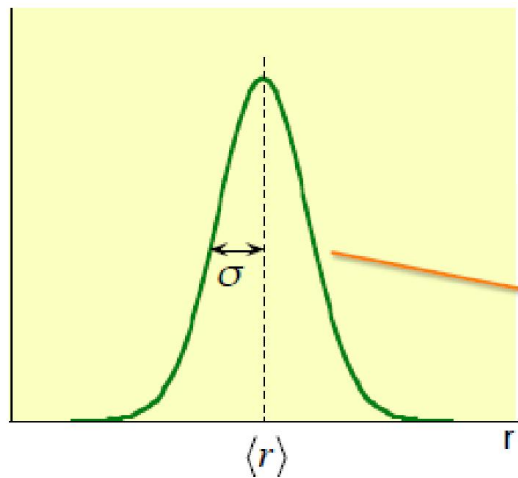Non-crystalline systems
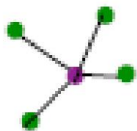
e.g.: a-Ge
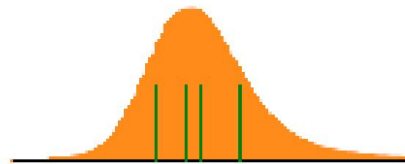
Nano-structures
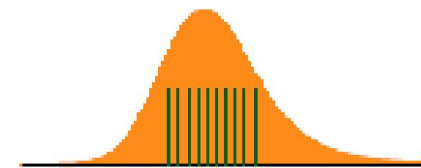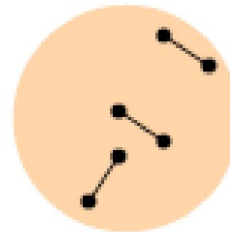
Free-volume models
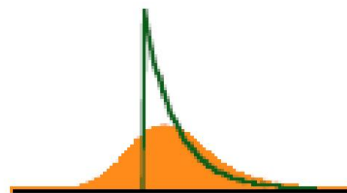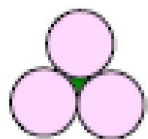
Enlarged distributions of distances

Thermal + Structural Disorder = Distribution of distances
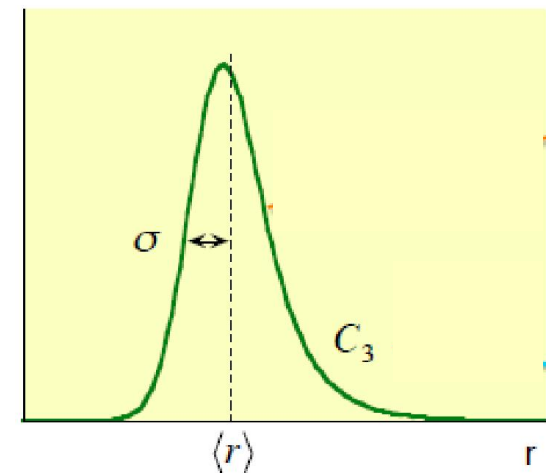
Simplest Model – Gaussian approximation

Asymmetric Distribution

$$P(r,\lambda) = \frac{1}{\sigma\sqrt{2\pi}} \exp\left[\frac{(r-\langle r\rangle)^2}{2\sigma^2}\right]$$

$$\sigma^2 = \left\langle (r-\langle r\rangle)^2 \right\rangle$$

$$\langle r\rangle_{eff} = \langle r\rangle_{real} - \frac{2\sigma^2}{\langle r\rangle}\left(1 - \frac{\langle r\rangle}{\lambda}\right)$$

$$C_3 = \left\langle (r-\langle r\rangle)^3 \right\rangle$$

Third cumulant
Asymmetry parameter

$$\sin\left[2kR_j + \frac{4}{3}k^3 C_3 + \delta_j(k)\right]$$

$$\chi(k) = \sum_j \frac{N_j f_j(k) e^{-2k^2\sigma_j^2}}{kR_j^2} \sin[2kR_j + \delta_j(k)]$$

Using a damped wave-function: $\boxed{e^{ikr} e^{-r/\lambda(k)}/kr}$ where $\lambda(k)$ is the photo-electron's *mean free path* (including core-hole lifetime), the EXAFS equation becomes:

$$\chi(k) = \sum_j \frac{N_j f_j(k) e^{-2R_j/\lambda(k)} e^{-2k^2\sigma_j^2}}{kR_j^2} \sin[2kR_j + \delta_j(k)]$$

Another important Amplitude Reduction Term is due to the relaxation of all the other electrons in the absorbing atom to the hole in the core level:

$$S_0^2 = |\langle \Phi_f^{N-1} | \Phi_0^{N-1} \rangle|^2$$

$$0.7 < S_0^2 < 1.0$$

$$\chi(k) = \sum_j \frac{N_j S_0^2 f_j(k) e^{-2R_j/\lambda(k)} e^{-2k^2\sigma_j^2}}{kR_j^2} \sin[2kR_j + \delta_j(k)]$$

If we know the *scattering* properties of the neighboring atom: $f(k)$ and $\delta(k)$, and the mean-free-path $\lambda(k)$ we can determine:

R distance to neighboring atom.

N coordination number of neighboring atom.

σ^2 mean-square disorder of neighbor distance.

The scattering amplitude $f(k)$ and phase-shift $\delta(k)$ depend on atomic number, so that XAFS is also sensitive to Z of the neighboring atom.
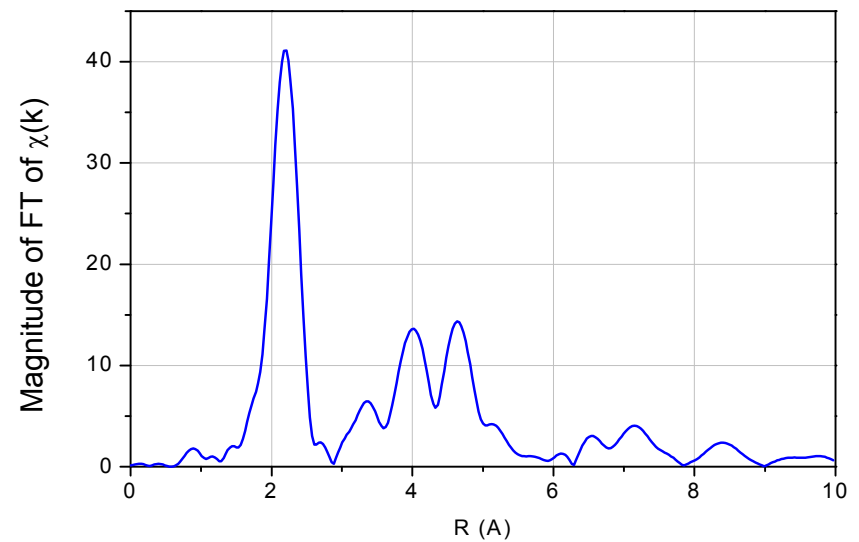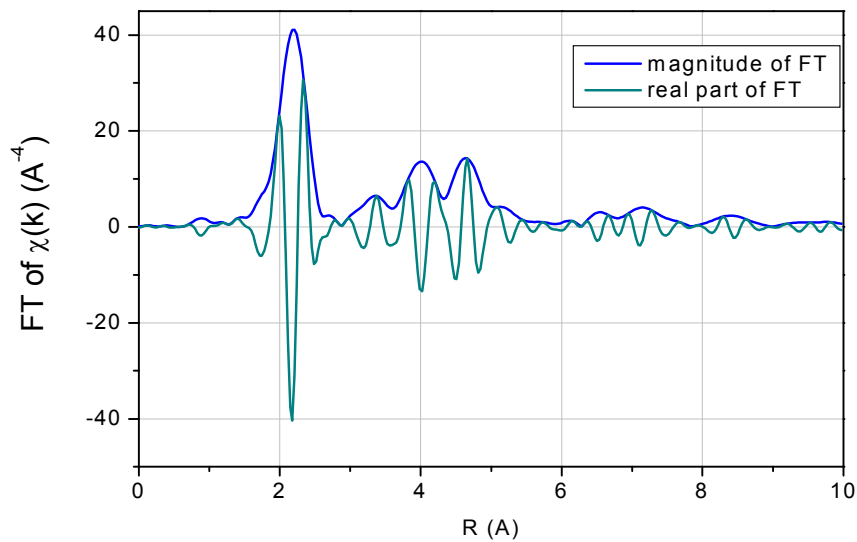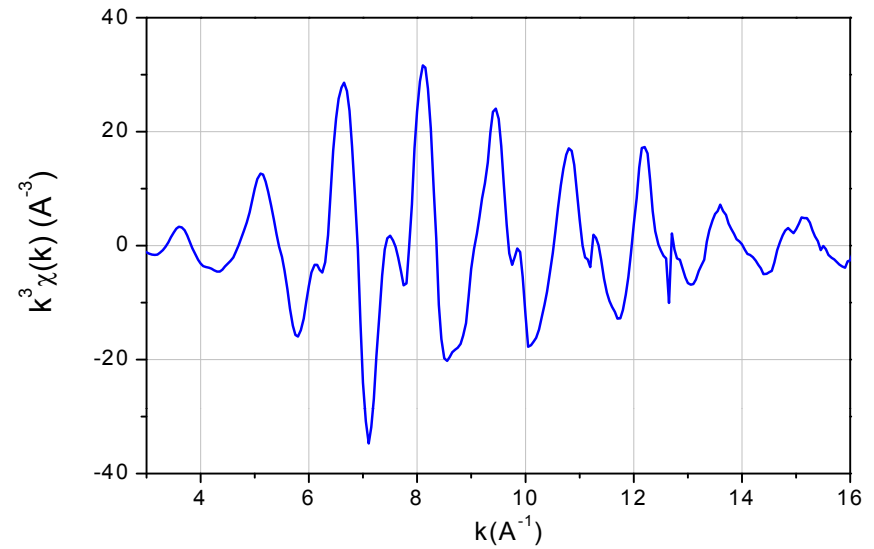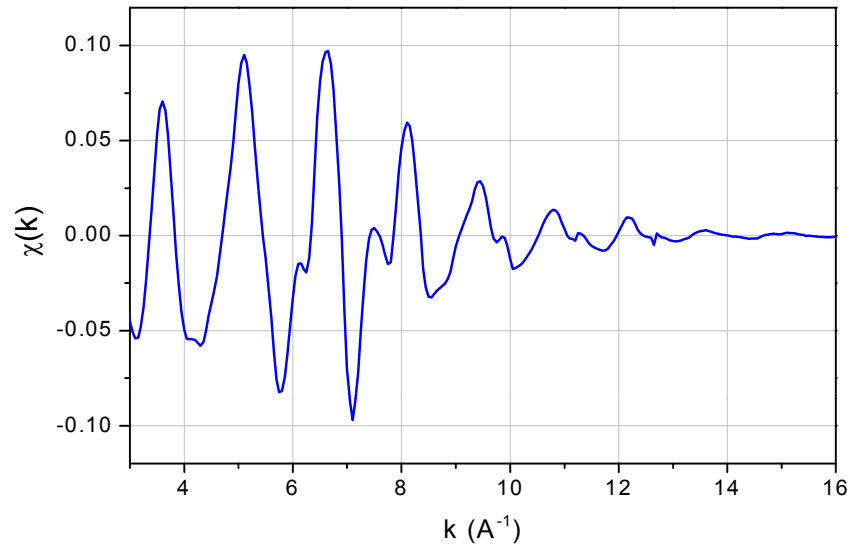
XAFS: Experiment
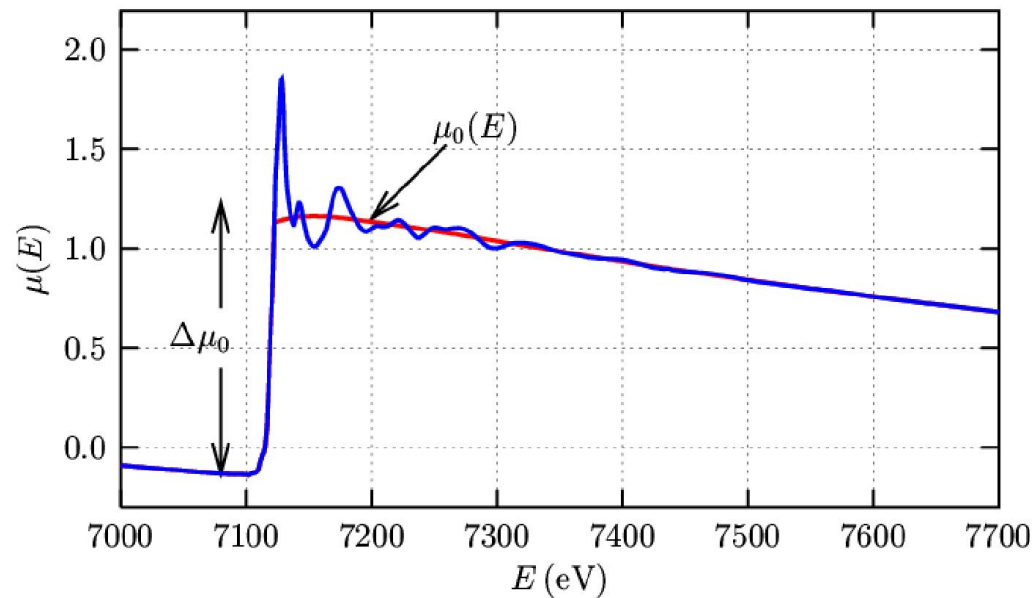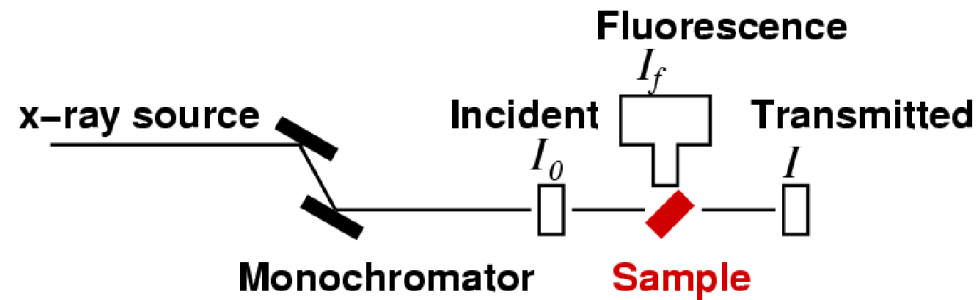
$$I = I_0 \exp(-\mu t) \quad or \quad \mu(E) = ln(I_0/I)$$
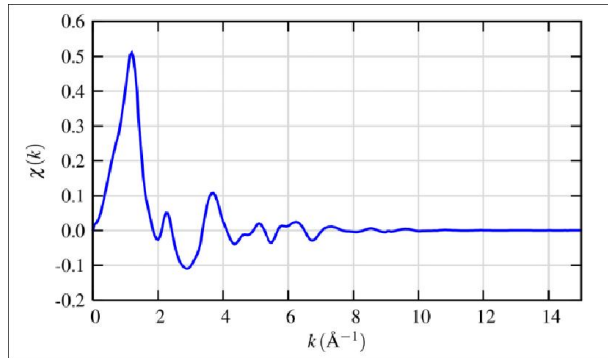
$$\chi(E) = \frac{\mu(E) - \mu_0(E)}{\Delta\mu_0(E_0)}$$

Background Subtraction and Normalization
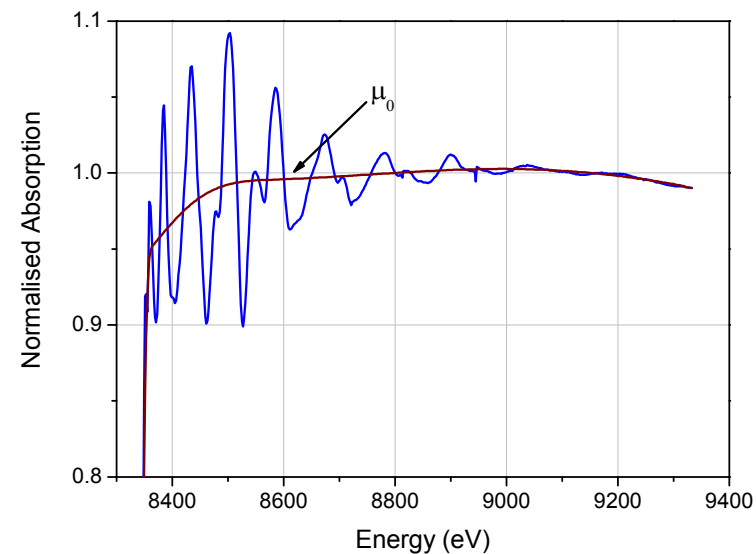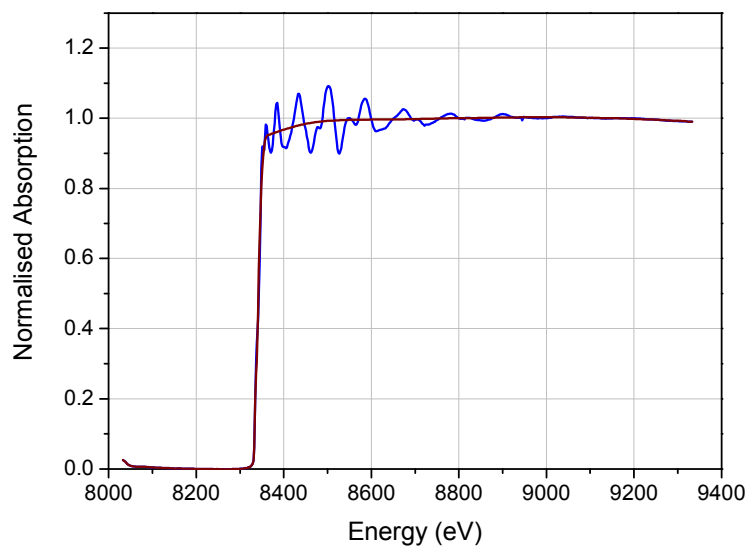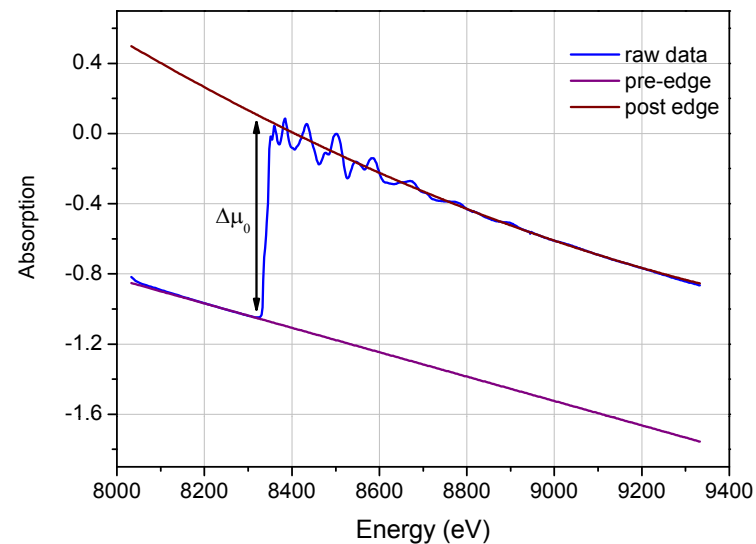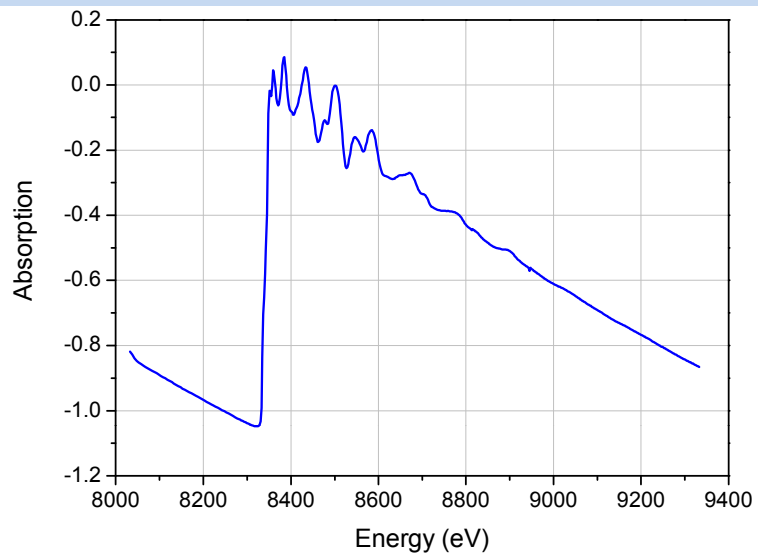
EXAFS: χ(k), k weighting and χ(R)
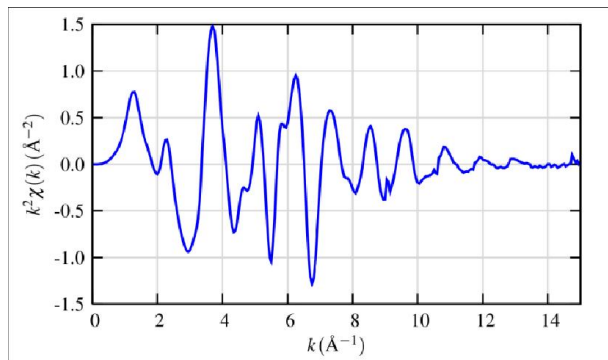
EXAFS: χ(k)

XAFS is an interference effect and depends on wave nature of photo-electron.

$$k = \sqrt{\frac{2m(E - E_0)}{\hbar^2}}$$

To model the EXAFS, we use EXAFS equation,

$$\chi(k) = \sum_j \frac{N_j S_0^2 f_j(k) e^{-2R_j/\lambda(k)} e^{-2k^2\sigma_j^2}}{kR_j^2} \sin\left[2kR_j + \delta_j(k)\right]$$

where *f(k)* and *δ(k)* are photo-electron scattering properties of the neighbouring atoms.

If we know these properties then we can determine,
N – coordination number of neighbouring atom
R – distance to neighbouring atom
σ² – mean square disorder of neighbour distance

Data Modeling

- Done using a guess structure, chemical plausibility and any other information.

- The number of parameters that can be determined is given by

$$N = \frac{2\Delta k \Delta R}{\pi}$$

  where Δk and ΔR are usable ranges of EXAFS in k and R space respectively. Typically Δk = [3 to 14 Å^{-1}] and ΔR = [1 to 5Å] which gives about 23 parameters.

- The R, N and σ^2 for different paths can be constrained to reduce the number of parameters.

Errors

- Random Experimental Fluctuations

- Systematic Errors
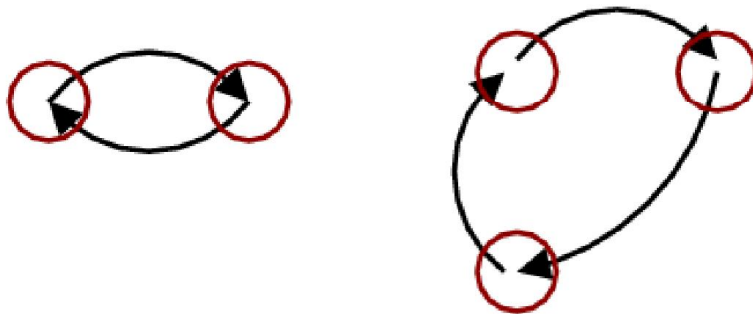
- Statistical uncertainties of data analysis

δX
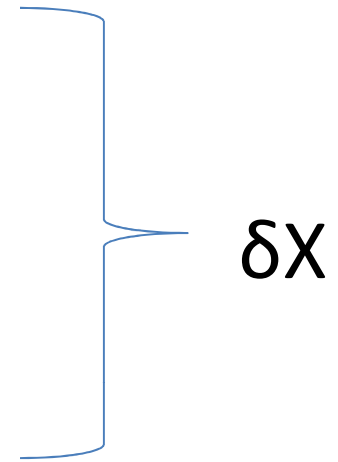
$$X \pm \delta X$$

- **Repeat the Experiment**

Scattering Paths

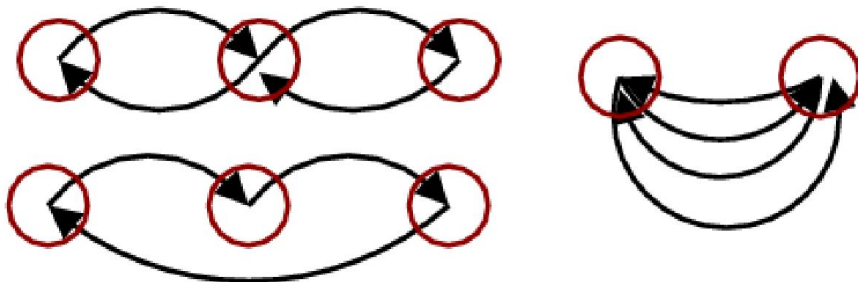- A model (guess structure) is required to calculate *f(k)* – scattering amplitude and *δ(k)* – phase shift.

Single Scattering Triangle Paths

Focussed Multiple Scattering Paths

Triangle paths 45 < θ < 135 aren't strong but there can be a lot of them.
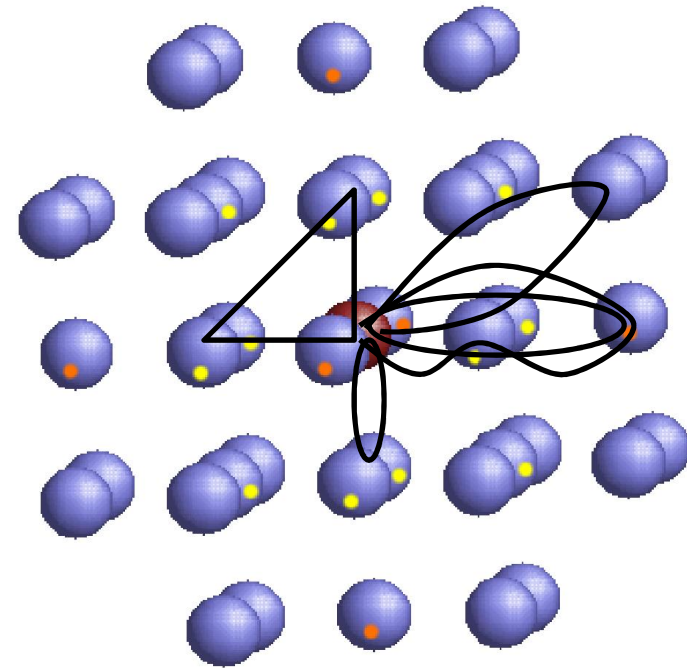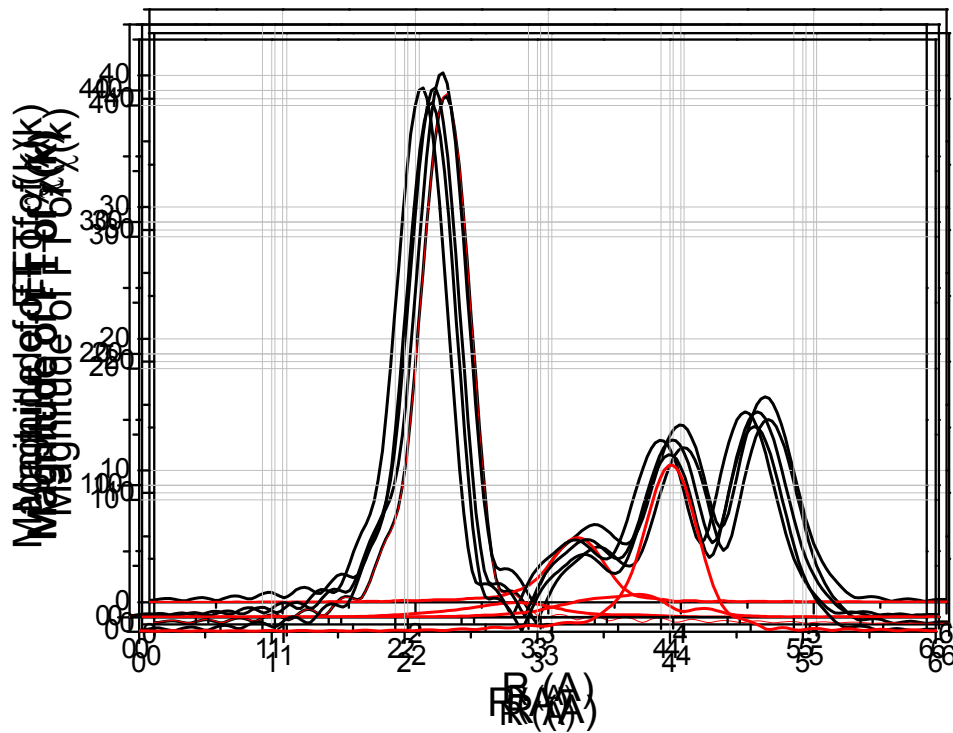
Multiple scattering paths with θ ≈ 180 are very strong.

Angular dependence of scattering can be used to estimate bond angles.

Ni Metal (Example)

- Ni metal has face centered cubic structure with a = 3.523Å.

Ni metal: R-space fitting
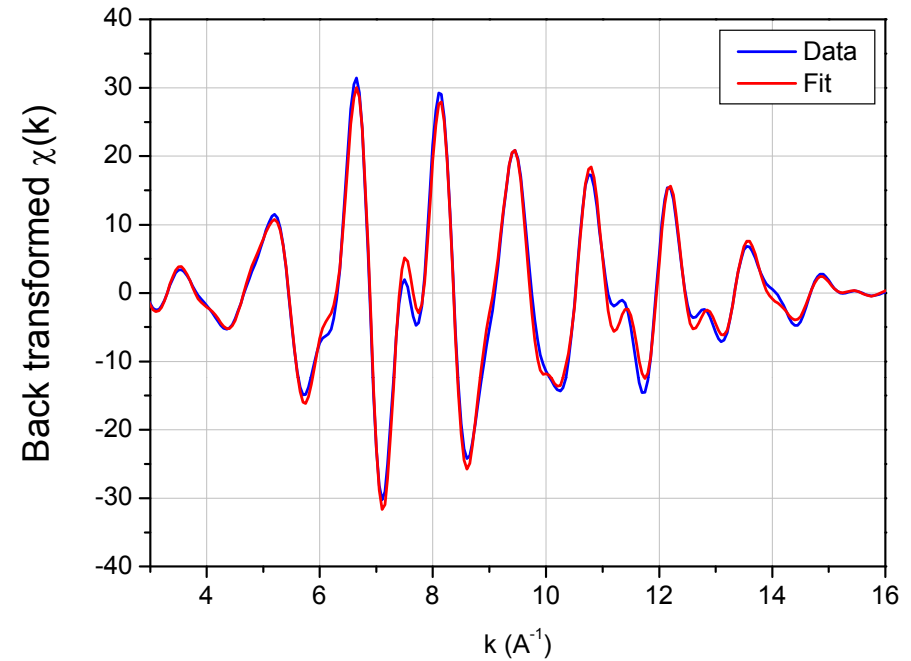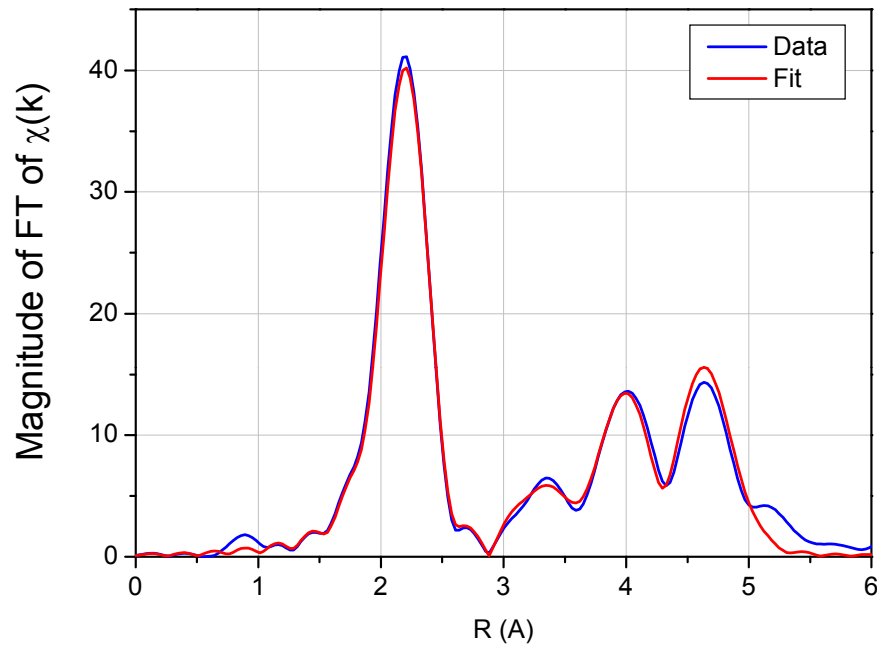
| Shell	N	R (Å)	σ^2 (Å^2)
Ni-Ni	12	2.488(.008)	0.0063(.0004)
Ni-Ni	6	3.52(.01)	0.009(.001)
Ni-Ni-Ni	48	3.73(.01)	0.012(.001)
Ni-Ni-Ni	48	4.25(.01)	0.007(.001)
Ni-Ni	24	4.31(.01)	0.009(.001)

Nickel Oxide (NiO)

- NiO has rock salt structure with a lattice parameter of 4.177Å.

- Nearest neighbour – 6 O at 2.088Å and
  second neighbour – 12 Ni at 2.953Å.
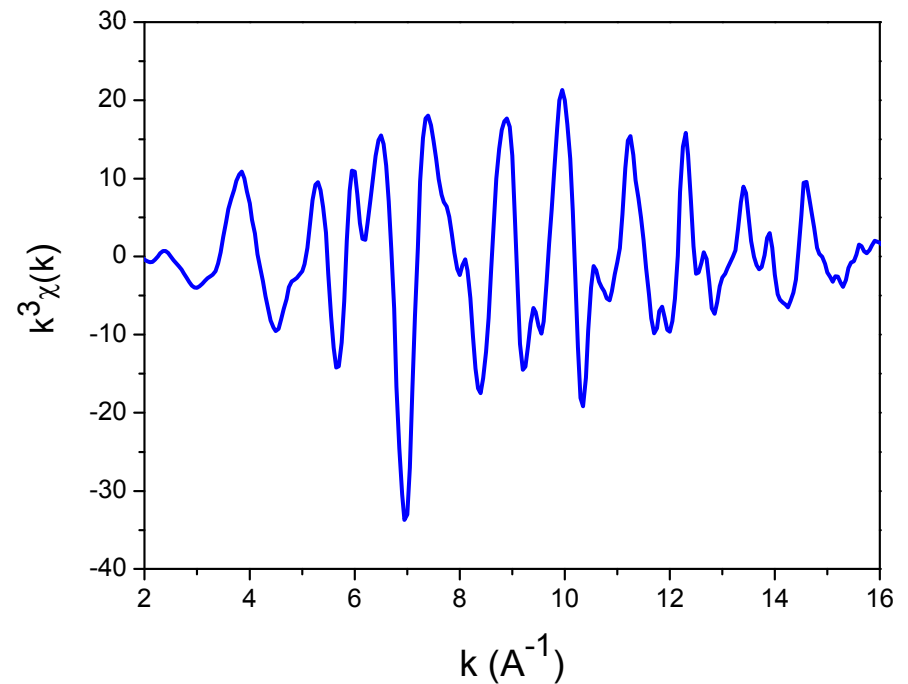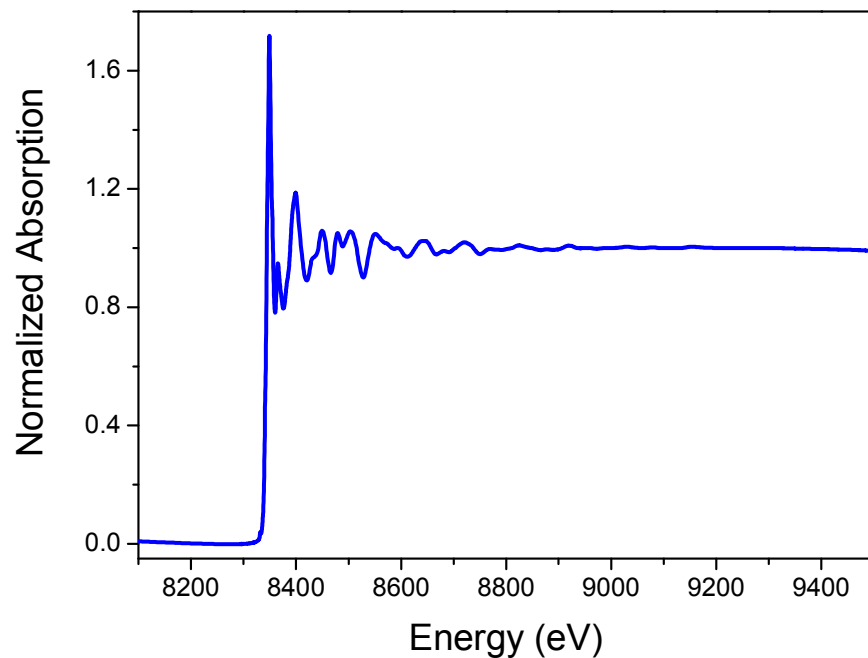
NiO EXAFS modeling

- To model NiO EXAFS we calculate the scattering amplitude f (k) and phase-shift δ(k), based on a guess of the structure, with Ni-O distance R = 2.08Å.
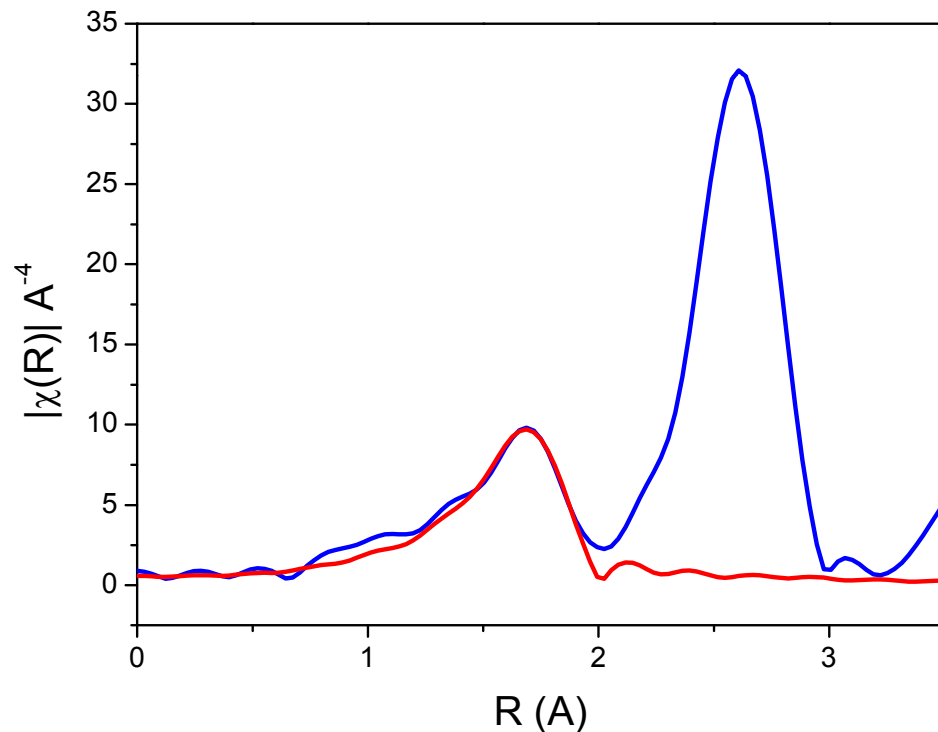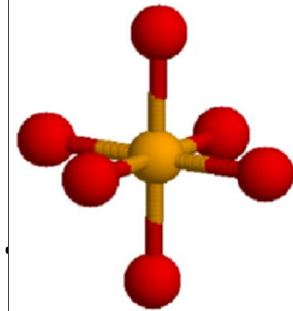
Fit results

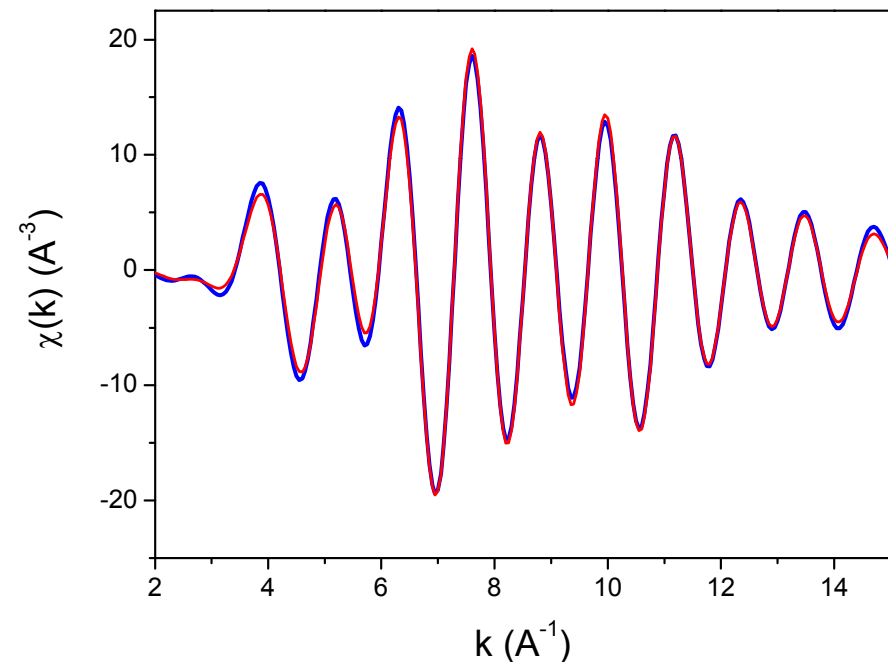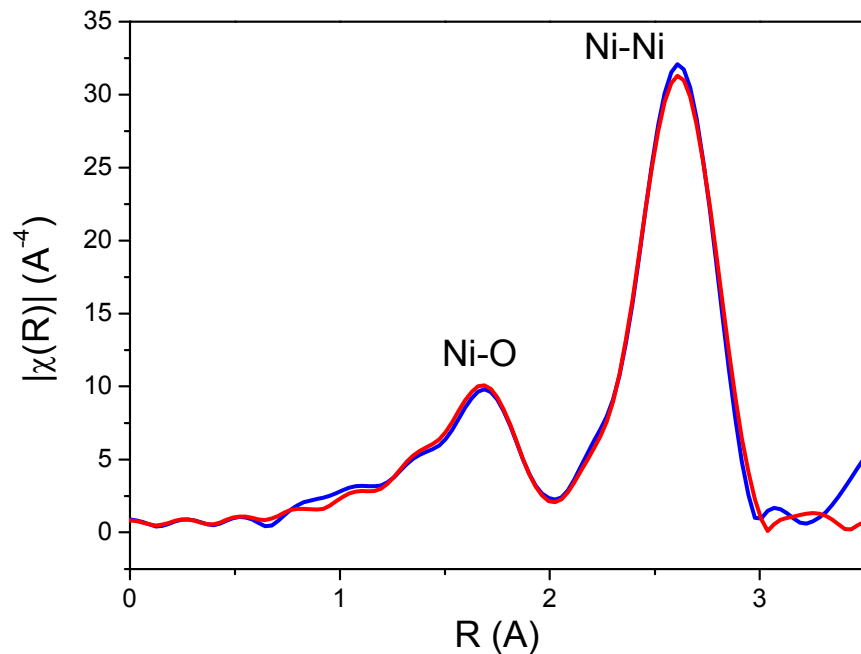N = 5.3 ± 0.7
R = 2.075 ± 0.005Å
σ^2 = 0.0055 ± 0.0007Å².

- To adding the second shell Ni to the model, we use calculation for f (k) and δ(k) based on a guess of the Ni-Ni distance, and refine the values R,N, σ^2. Such a fit gives a result like this:

| Shell	N	R (Å)	σ^2 (Å^2)
Ni-O	6.0(1.0)	2.10(.02)	0.0058(.0001)
Ni-Ni	11.4(0.7)	3.05(.02)	0.0059(.0003)

XANES

- XANES is the region of X-ray absorption spectrum within about 50 eV of the absorption edge.

XANES is strongly sensitive to chemistry (formal oxidation state and geometry) of absorbing atom.
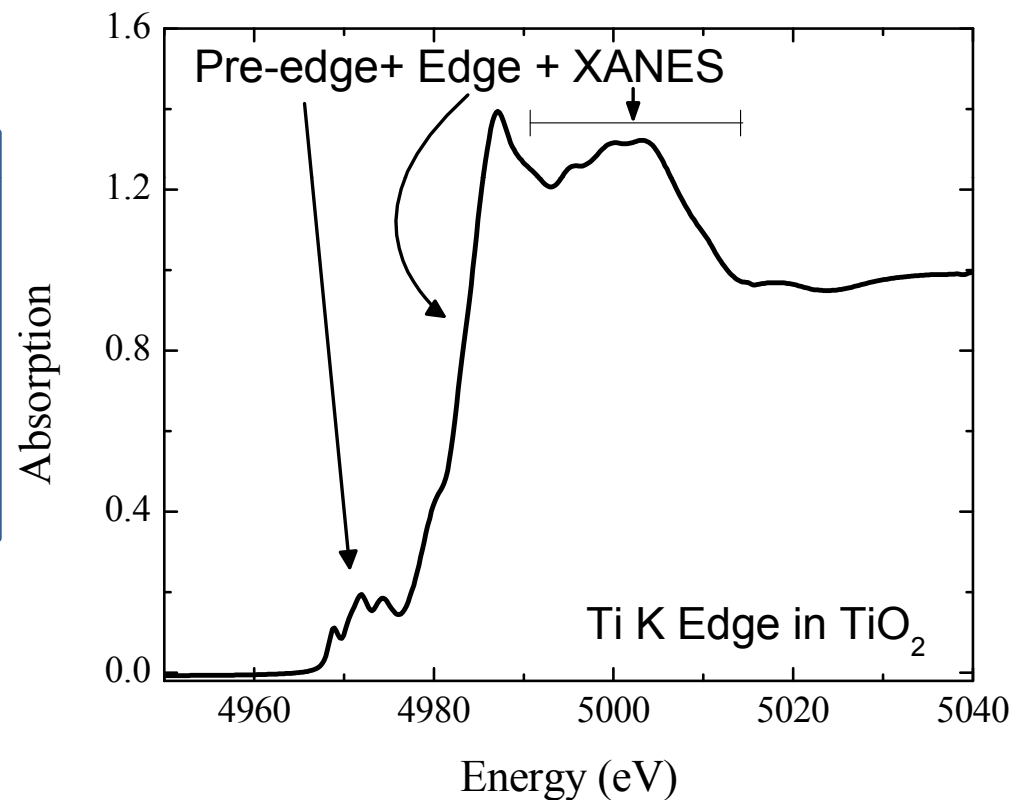
Region	Transitions	Information Content
Pre-edge	Features caused by electronic transitions to empty bound states. Transition probability controlled by dipolar selection rules.	Local geometry around absorbing atom. Dependence on oxidation state and bonding characteristics (chemical shift).
Edge	Defines ionization threshold to continuum states.	Dependence on oxidation state (chemical shift), main edge shifts to higher energy with increased oxidation state. (As much as 5 eV per one unit change).
XANES	Features dominated by multiple-scattering resonances of the photoelectrons ejected at low kinetic energy. Large scattering cross section.	Atomic position of neighbors: interatomic distances and bond angles. Multiple scattering dominates but *ab initio* calculations providing accessible insight (e.g. FEFF8).
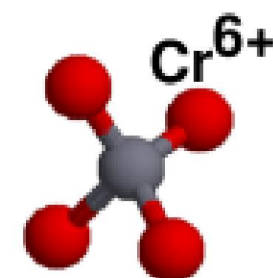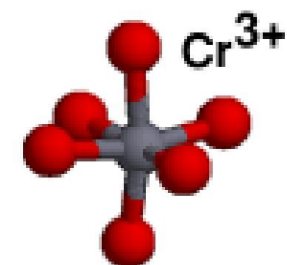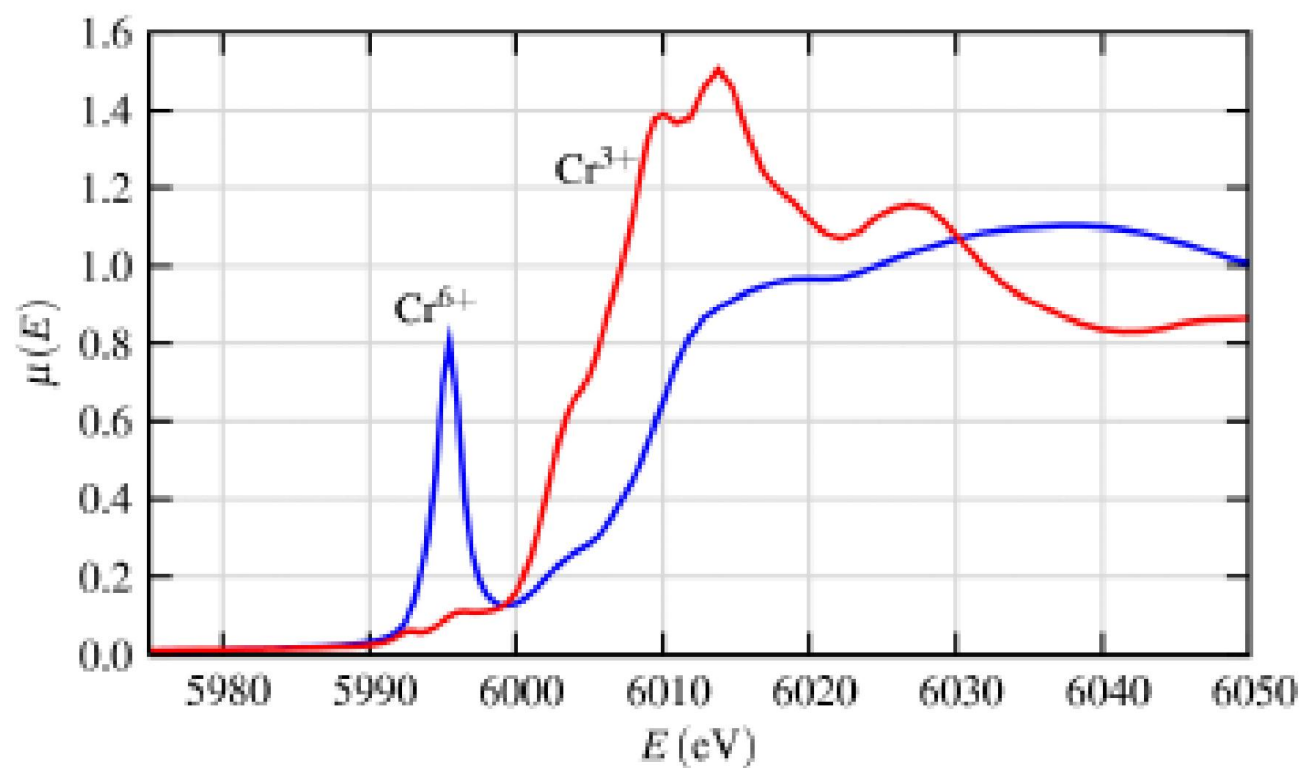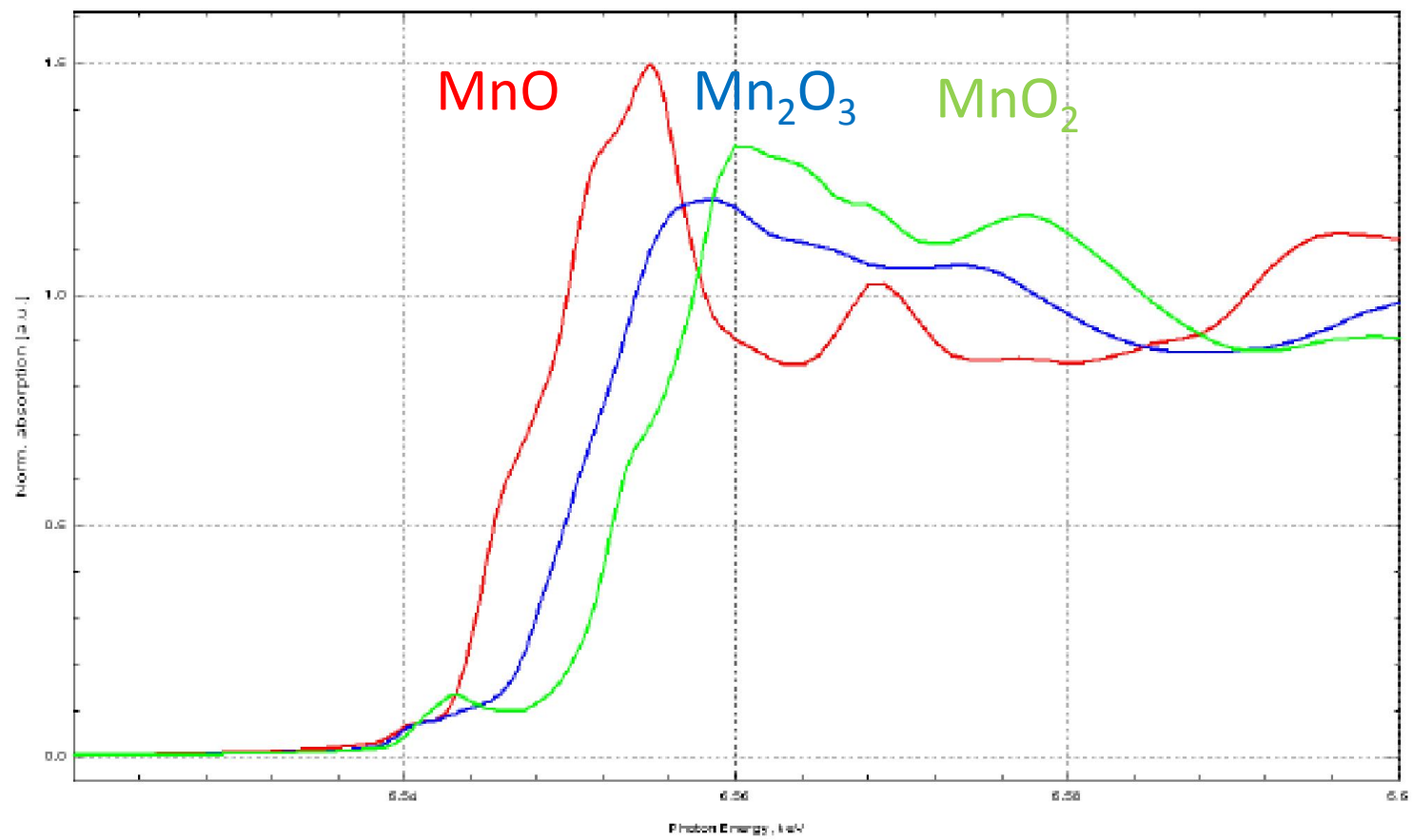
XANES Interpretation

The EXAFS Equation breaks down at low-k, and the mean-free-path goes up. This complicates XANES interpretation:

> *We do not have a simple equation for XANES.*

XANES can be described *qualitatively* (and nearly *quantitatively*) in terms of

coordination chemistry	regular, distorted octahedral, tetrahedral, ...
molecular orbitals	p-d orbital hybridization, crystal-field theory, ...
band-structure	the density of available electronic states.
multiple-scattering	multiple bounces of the photo-electron.

These chemical and physical interpretations are all related, of course:

> **What electronic states can the photo-electron fill?**

XANES calculations are becoming reasonably accurate and simple. These can help explain what *bonding orbitals* and/or *structural characteristics* give rise to certain spectral features.

Quantitative XANES analysis using first-principles calculations are still rare, but becoming possible...
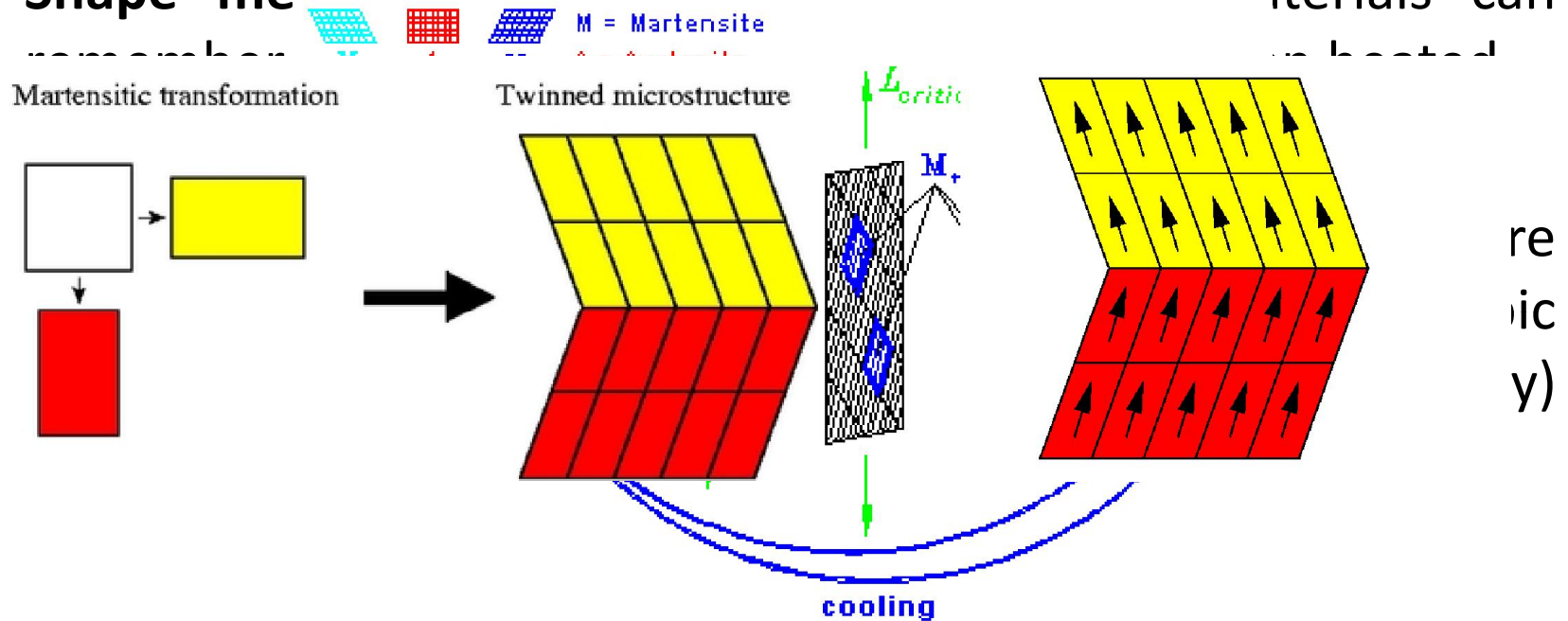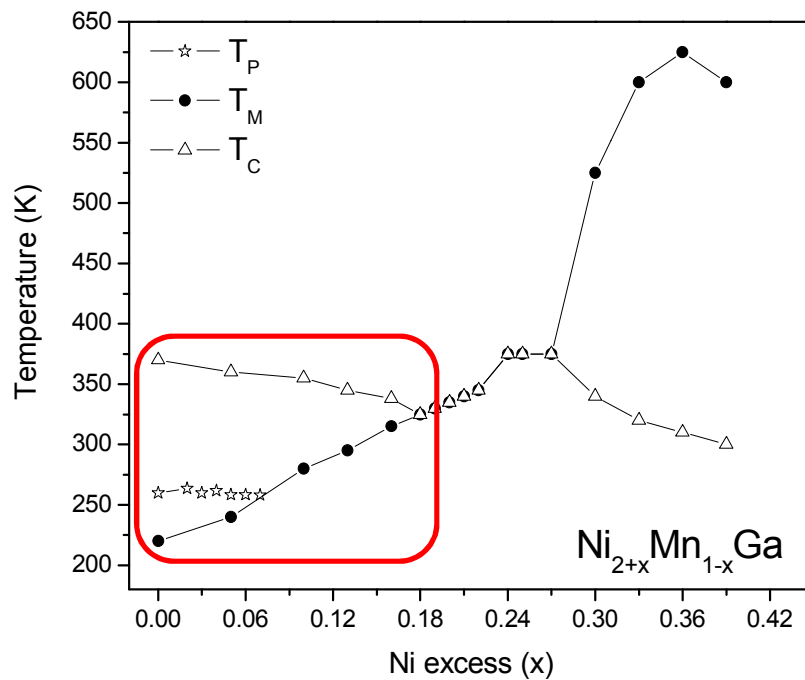
Shape Memory Alloys

Introduction

- **Shape memory** - After deformation these materials can remember ~~when heated~~

- re ...ic ...y)

- The transformation can be influenced by temperature, pressure and magnetic field.

Ni$_2$MnGa - series

- **Ni$_2$MnGa** – Ferromagnetic T$_C$ = 375K

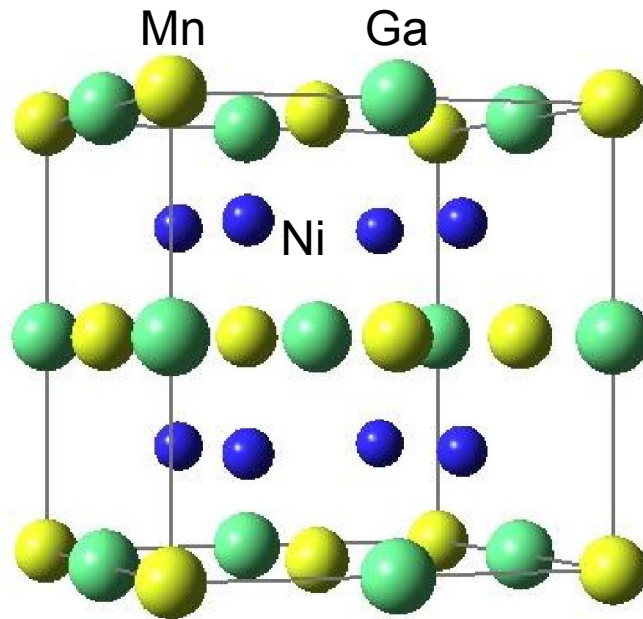 Martensitic Transformation T$_M$ = 220K

In Ni$_{2+x}$Mn$_{1-x}$Ga, up to x = 0.19 T$_M$ increases and T$_C$ decreases.
We have studied XAFS at Mn and Ga K edges in x = 0, 0.1, 0.13, 0.16 and 0.19.

Crystal Structure

- Austenitic Phase – Cubic, $L2_1$ ordered Heusler (X_2YZ) structure

- Martensitic Phase – 5M/7M – 5 layer or 7 layer modulations of(110) planes along$[1\bar{1}0]$ direction.

  – V. V. Matrynov and V. V. Kokorin, J. de Phys III **2** 739 (1992)
  – J. Pons *et al*, Acta Mater. **48** 3027 (2000);

               J. Appl. Phys. **97** 083516 (2005)
  – P. J. Brown *et al* JPCM **14** 10159 (2002)
  – S. Banik *et al* Phys. Rev. B **75** 104107 (2007).
  – R. Ranjan et al Phys. Rev. B. **74** 224443 (2006).
  – L. Righi et al Acta Mater. **55** 5237 (2007).

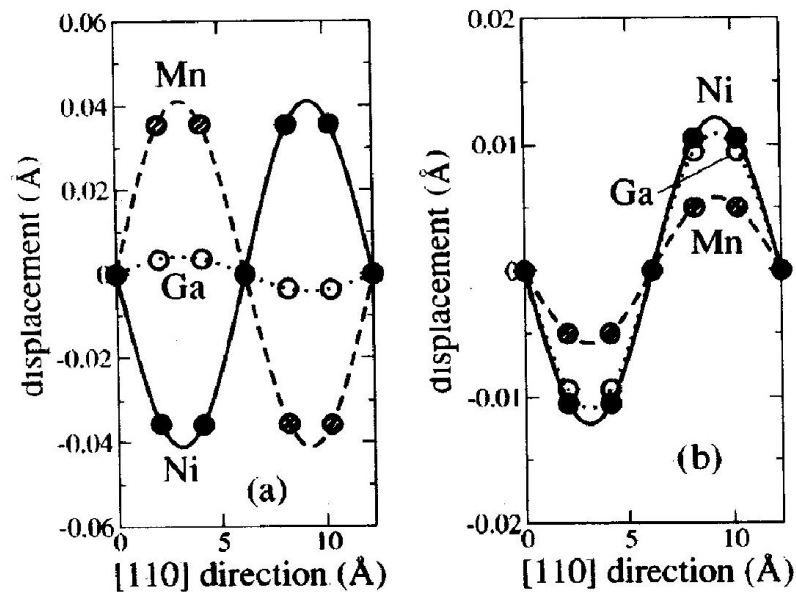   Acta Mater. **56** 4529 (2008).
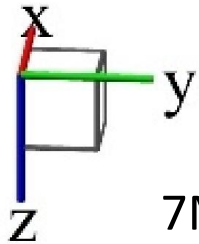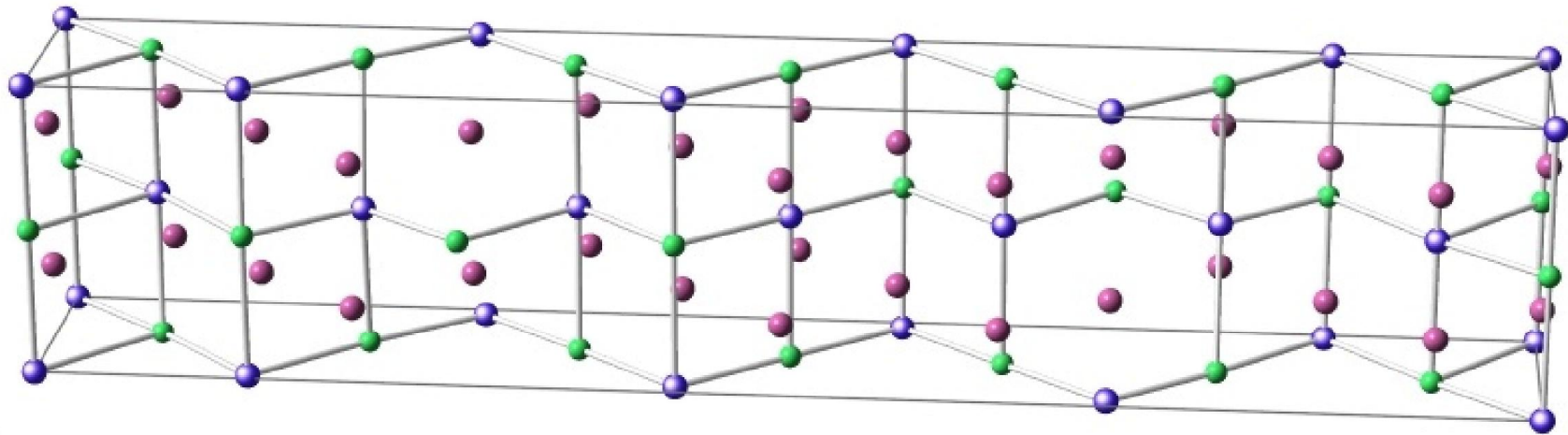
Brown *et.al*. J. Phys.:Condens. Matter 14 10159 (2002)

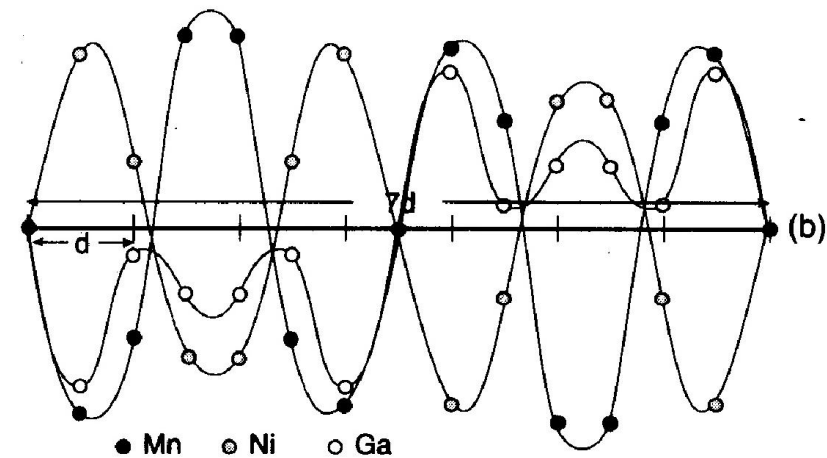7M commensurate orthorhombic structure with sinusoidal modulations

XRD studies based on superspace approach reported an incommensurate structure with $q_B = 0.4248$.

Possible Scenario for Modulations

Theory
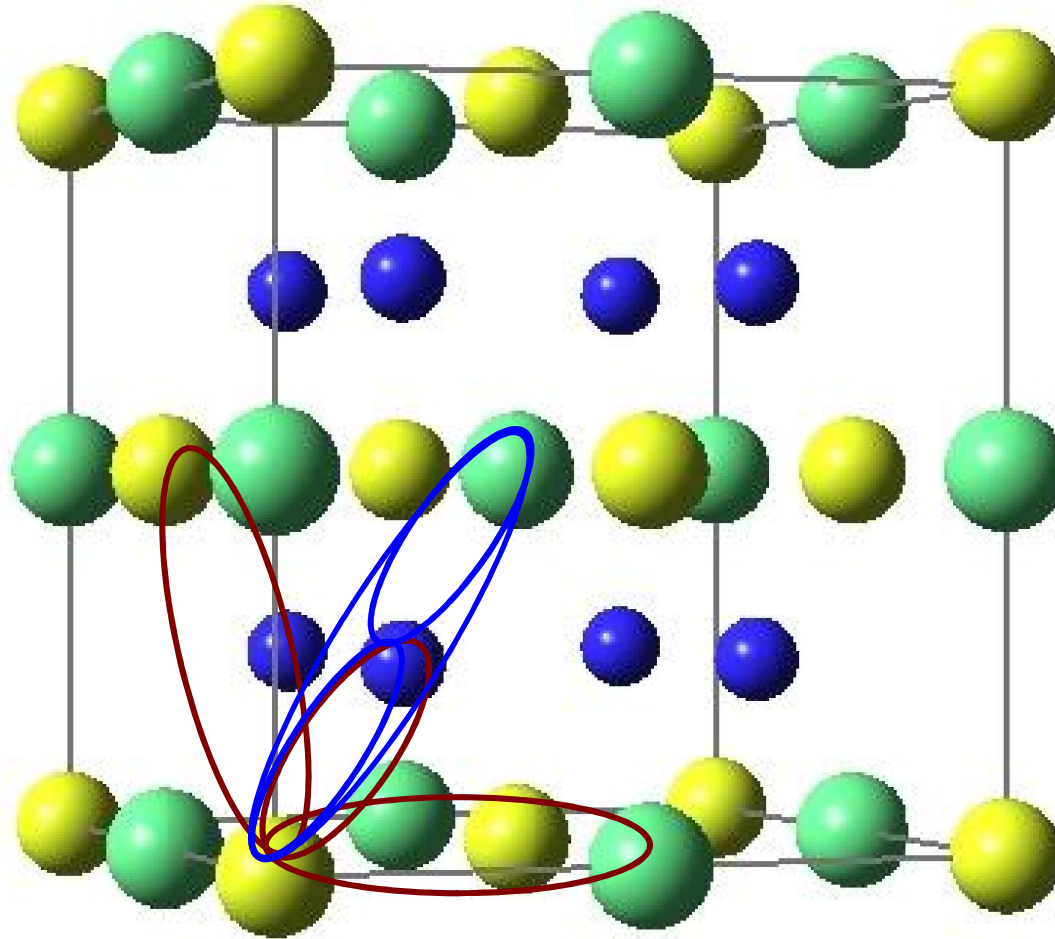
Experiment

Zayak *et. al* Phys. Rev. B 68, 132402 (2003)

Brown *et.al*. J. Phys.:Condens. Matter 14 10159 (2002)

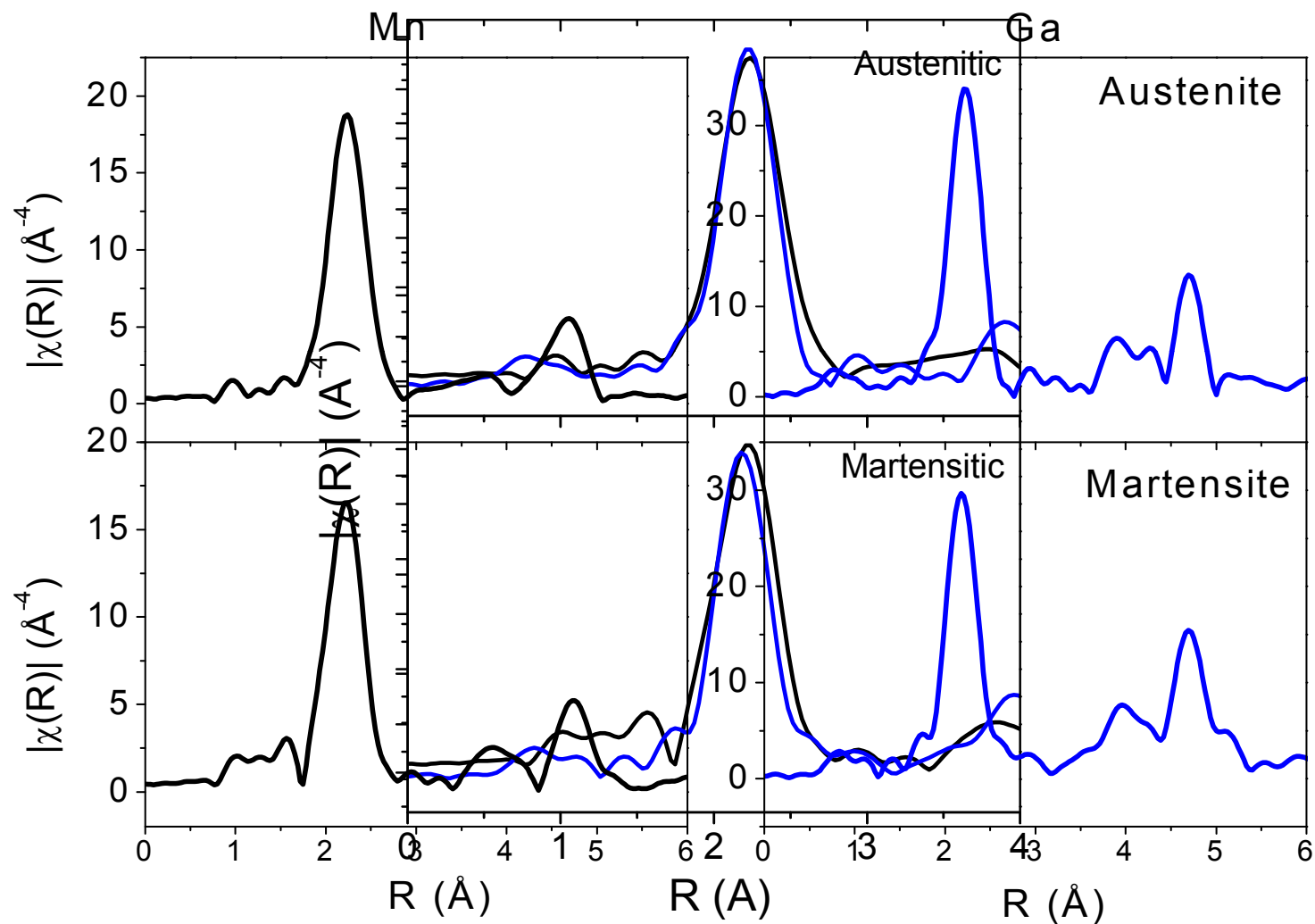For x ≥ 0.18, a non modulated tetragonal structure is reported.

Experiment

- EXAFS at Mn and Ga K edge were performed at XAFS beamline at Elettra.

- Sample – powder on tape.

- Two temperatures – R.T. (austenitic) and at Liquid Nitrogen temperature (martensitic).
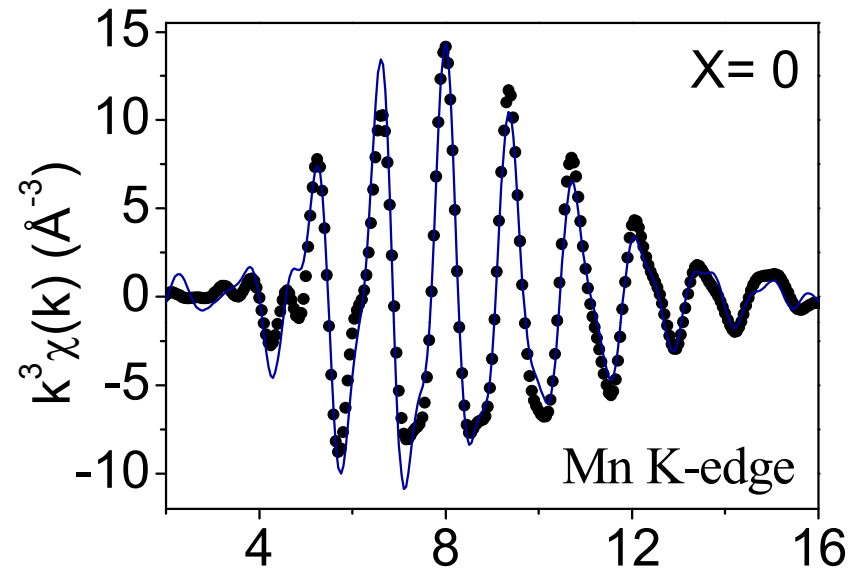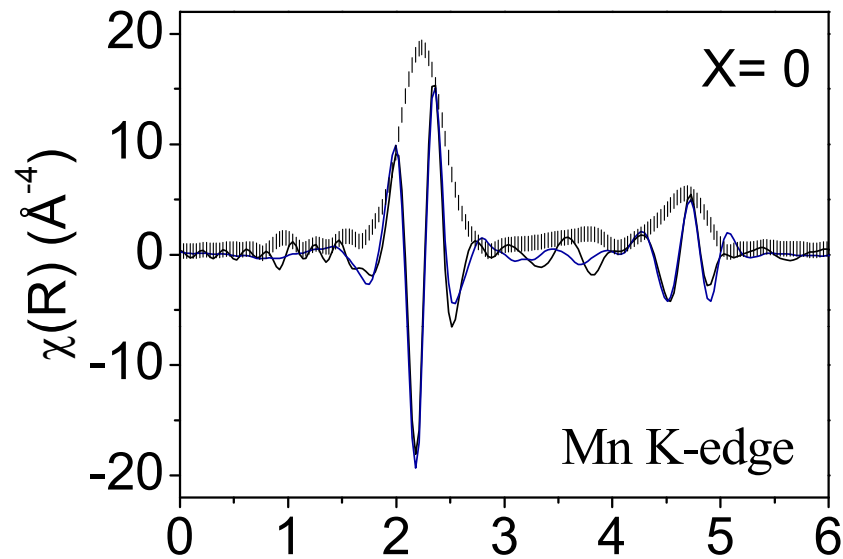
L2$_1$ Heusler Structure

Ni$_2$MnGa: FT of Mn and Ga XAFS

Mn K-edge EXAFS at RT in Ni$_2$MnGa
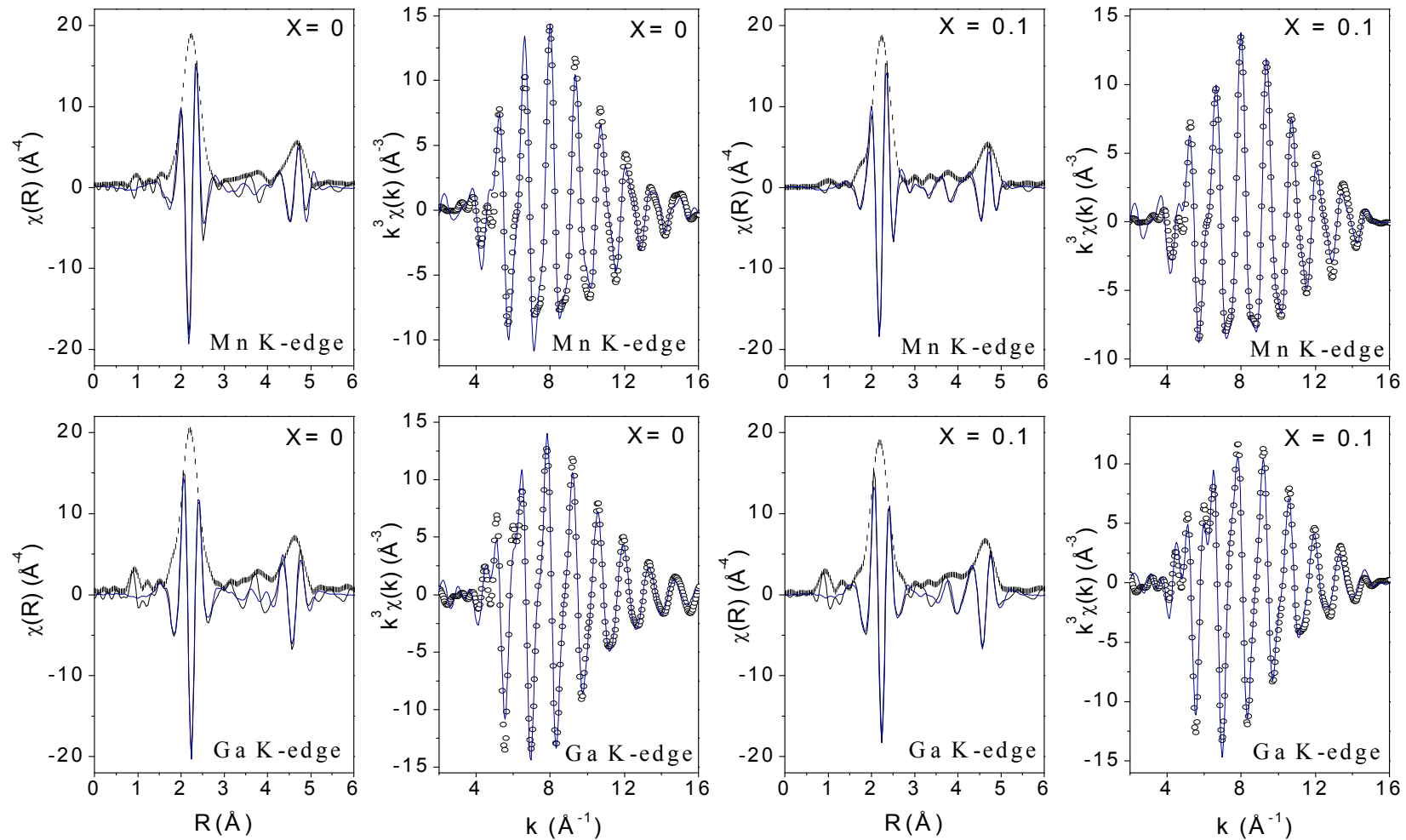

Magnitude and real component fitting in R space and back transformed *k* space

k range = (2 – 15) Å^{-1} ;   *k* weight = 3;   R range = (1 - 5) Å

Magnitude and Real component fitting of Mn and Ga K-edge EXAFS at RT in x = 0, 0.1

k range = (2 – 15) Å⁻¹ ;   *k* weight = 3;   R range = (1 - 5) Å

Results of the fits to the RT Mn K-edge data

Atom and	X = 0		X = 0.1	
Coord.No.	R(Å)	σ^2(Å^2)	R(Å)	σ^2(Å^2)
Ni1 x 8	**2.513(2**)	0.0081(3)	2.512(2)	0.0080(2)
Ga1 x 6	2.909(3)	0.03(1)	2.795(8)	0.014(1)
Mn1 x 12	4.114(4)	0.029(9)	4.20(2)	0.021(3)
Ni2 x 24	4.824(5)	0.019(3)	4.85(1)	0.019(2)
Ga2 x 16	5.028(5)	0.007(1)	4.900(8)	0.008(1)
MS x 8	**5.024(5)**	0.0097(6)	5.02(1)	0.018(2)

MS ⟶ Mn – Ga3 – Ni1 - Mn

Numbers in the parentheses indicate uncertainty in the last digit

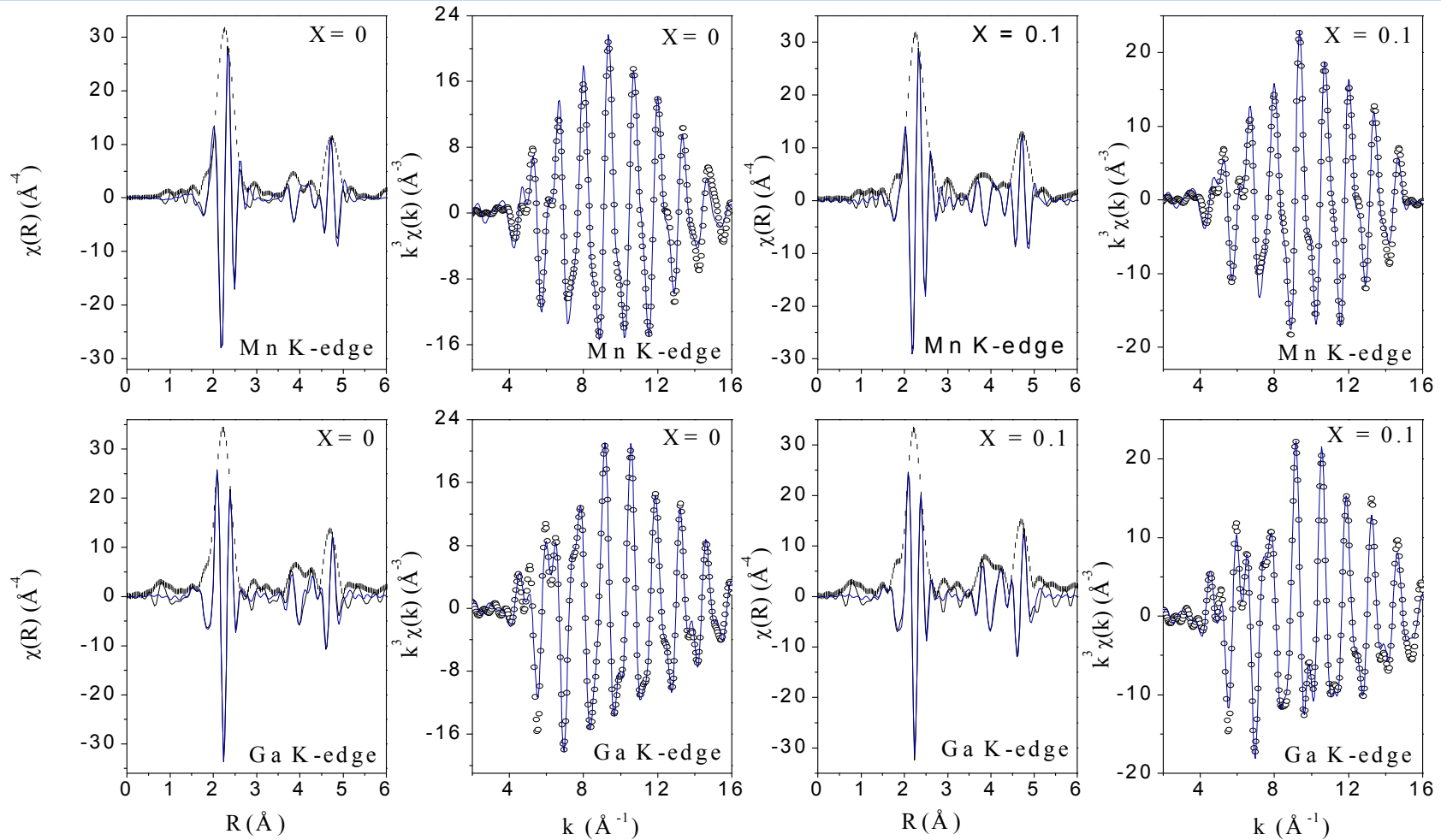# Results of the fits to the RT Ga K-edge data

Atom and Coord.No.	X = 0		X = 0.1	
	R(Å)	σ^2(Å^2)	R(Å)	σ^2(Å^2)
Ni1 x 8	**2.512(2)**	0.0070(2); T$_M$ = 250K 2.510(3)		0.0082(4)
Mn1 x 6	2.901(2)	0.030(6)	2.88(5)	0.026(7)
Ga1 x 12	2.795(8) 4.103(3)	0.014(1) 0.022(4)	2.88(5) 4.23(4)	0.026(7) 0.017(5)
Ni2 x 24	4.811(4)	0.015(1)	4.79(1)	0.016(2)
Mn2 x 16	5.025(3)	0.017(1)	4.90(1)	0.007(1)
MS x 8	**5.025(3)**	0.014(1)	5.15(3)	0.023(4)

MS ⟶ Ga – Mn3 – Ni1 - Ga

Numbers in the parentheses indicate uncertainty in the last digit

Magnitude and Real component fitting of Mn and Ga K-edge EXAFS at LT in x = 0, 0.1
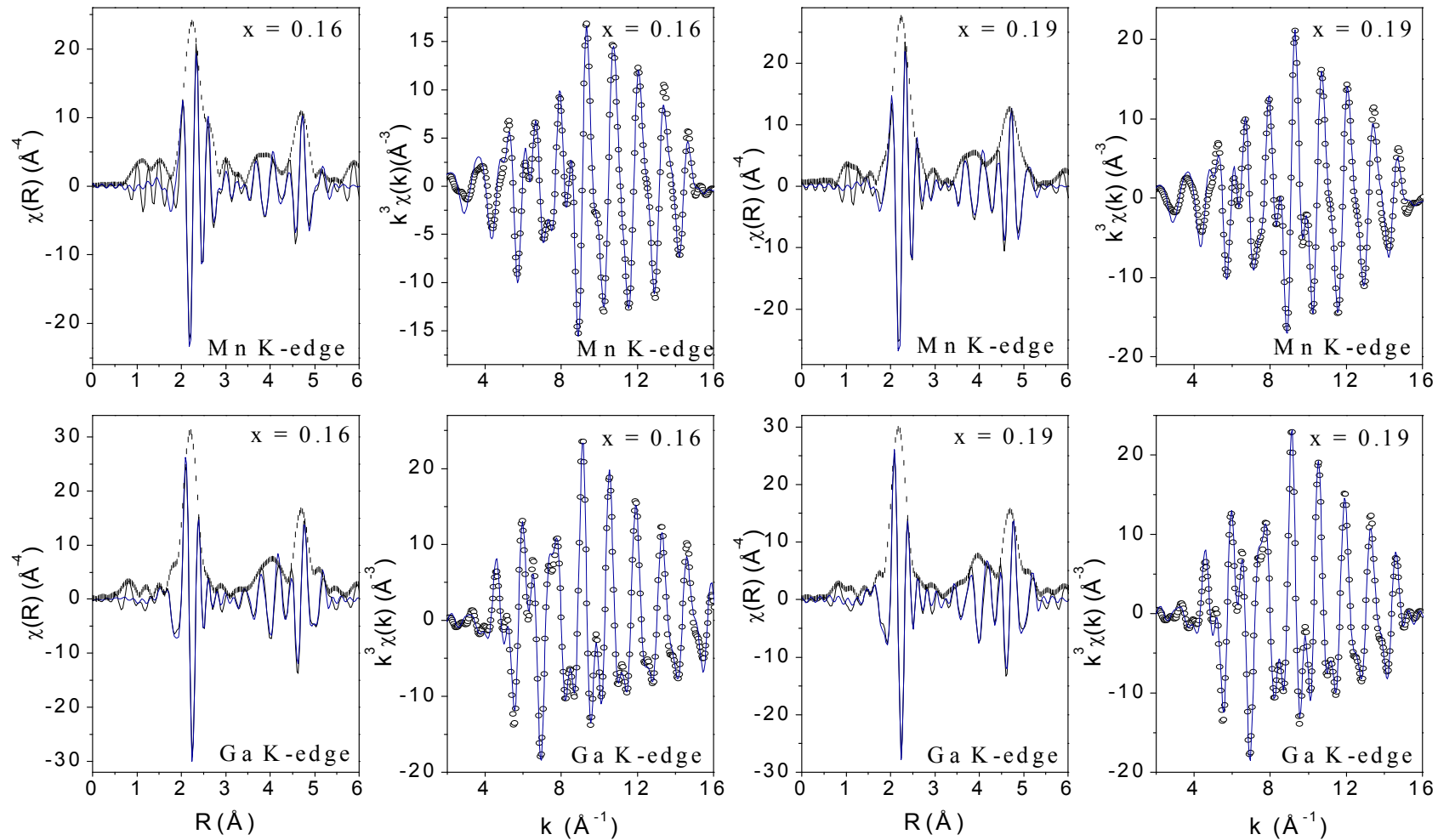

k range = $(2 – 15)$ Å^{-1} ;   *k* weight = 3;   R range = $(1 - 5)$ Å

Magnitude and Real component fitting of Mn and Ga K-edge EXAFS at LT in x = 0.16, 0.19

k range = (2 – 15) Å^{-1} ;   *k* weight = 3;   R range = (1 - 5) Å

Results of the fits to the LT Mn K-edge data

Atom and Coord.	X = 0		X = 0.1		X = 0.16		X = 0.19	
	R(Å)	σ²(Å²)	R(Å)	σ²(Å²)	R(Å)	σ²(Å²)	R(Å)	σ²(Å²)
Ni1 x 8	2.518(3)	0.0057(4)	2.518(5)	0.0056(5)	**2.523(2)**	0.0051(2)	2.521(2)	0.0081(2)
Ga1 x 4	2.780(6)	0.0043(5)	2.768(8)	0.0037(7)	2.739(3)	0.0054(3)	2.739(5)	0.0093(5)
Ga2 x 2	2.96(3)	0.008(3)	2.95(2)	0.009(2)	3.23(2)	0.012(3)	3.23(4)	0.03(1)
Mn1 x 4	3.96(3)	0.009(3)	3.93(3)	0.009(3)	3.89(3)	0.008(4)	3.93(3)	0.019(5)
Mn2 x 8	4.19(1)	0.009(2)	4.19(1)	0.009(2)	4.23(1)	0.011(1)	4.24(1)	0.012(1)
Ni2 x 16	4.69(1)	0.011(1)	4.66(1)	0.009(1)	4.61(1)	0.009(2)	4.60(1)	0.019(2)
Ni3 x 8	4.90(1)	0.006(1)	4.905(8)	0.0040(7)	5.327(8)	0.0044(8)	5.34(3)	0.0134(4)
MS x 16	5.068(6)	0.0095(7)	5.056(8)	0.0097(8)	5.075(4)	0.0068(4)	5.082(5)	0.0122(6)

MS ⟶ Mn – Ga3 – Ni1 - Mn

Results of the fits to the LT Ga K-edge data

Atom and Coord.	X = 0		X = 0.1		X = 0.16		X = 0.19	
	R(Å)	σ²(Å²)	R(Å)	σ²(Å²)	R(Å)	σ²(Å²)	R(Å)	σ²(Å²)
Ni1 x 8	2.5111(8)	0.00431(8)	2.512(2)	0.0044(2)	**2.511(1)**	0.0042(1)	2.512(2)	0.0074(2)
Mn1 x 4	2.791(4)	0.0078(5)	2.776(8)	0.0062(5)	2.722(4)	0.0067(5)	2.710(5)	0.0086(6)
Mn2 x 2	3.065(2)	0.012(2)	3.06(2)	0.013(4)	3.0(2)	0.03(3)	3.24(2)	0.016(9)
Ga1 x 4	3.97(1)	0.009(2)	3.93(2)	0.008(2)	3.85(2)	0.009(2)	3.85(3)	0.016(4)
Ga2 x 8	4.215(8)	0.0076(8)	4.214(9)	0.0079(9)	4.248(7)	0.009(1)	4.27(1)	0.011(1)
Ni2 x 16	4.706(8)	0.0048(6)	4.676(6)	0.0081(7)	4.619(7)	0.0083(6)	4.62(3)	0.023(4)
Ni3 x 8	4.889(3)	0.0047(3)	4.872(5)	0.0033(4)	5.319(8)	0.0025(5)	5.36(1)	0.007(1)
MS x 16	5.069(7)	0.0111(9)	5.111(5)	0.0089(6)	5.106(2)	0.0047(3)	5.131(1)	0.0104(6)

MS ⟶ Ga – Mn3 – Ni1 - Ga

Results of the fits: Mn and Ga K-edge data

For x = 0 and 0.1

Mn-Ga2 = 2.95(2)   Ga-Mn2 = 3.06(2)

For x = 0.13 and 0.16

Mn-Ga2 = 3.23(4)   Ga-Mn2 = 3.0(1)

For x = 0.19

Mn-Ga2 = 3.23(4)   Ga-Mn2 = 3.24(2)

Summary of EXAFS Results

- For x = 0, 0.1   For x = 0.13, 0.16

  Mn-Ga2 = 2.95(2) 0.009(2)   Mn-Ga2 = 3.23(4) 0.012(5)

  Ga-Mn2 = 3.06(2) 0.013(4)   Ga-Mn2 = 3.0(1)   0.03(2)

- Higher σ^2 for Ga as central atom in comparison to Mn

- Mn-Ni + Ga-Ni = Multiple Scattering path,   the planes are

  2.518 + 2.511 = 5.029 ≠ 5.069   "dimpled"

- Mn-Ni = 2.523(2) and 0.0051(1)   a difference of 0.011 Å

  Ga-Ni = 2.511(1) and 0.0042(1)   Ga closer to Ni

L2$_1$ Heusler Structure
L1$_0^1$ sub cell

XANES Studies

Sathe et al JPCM (2013)
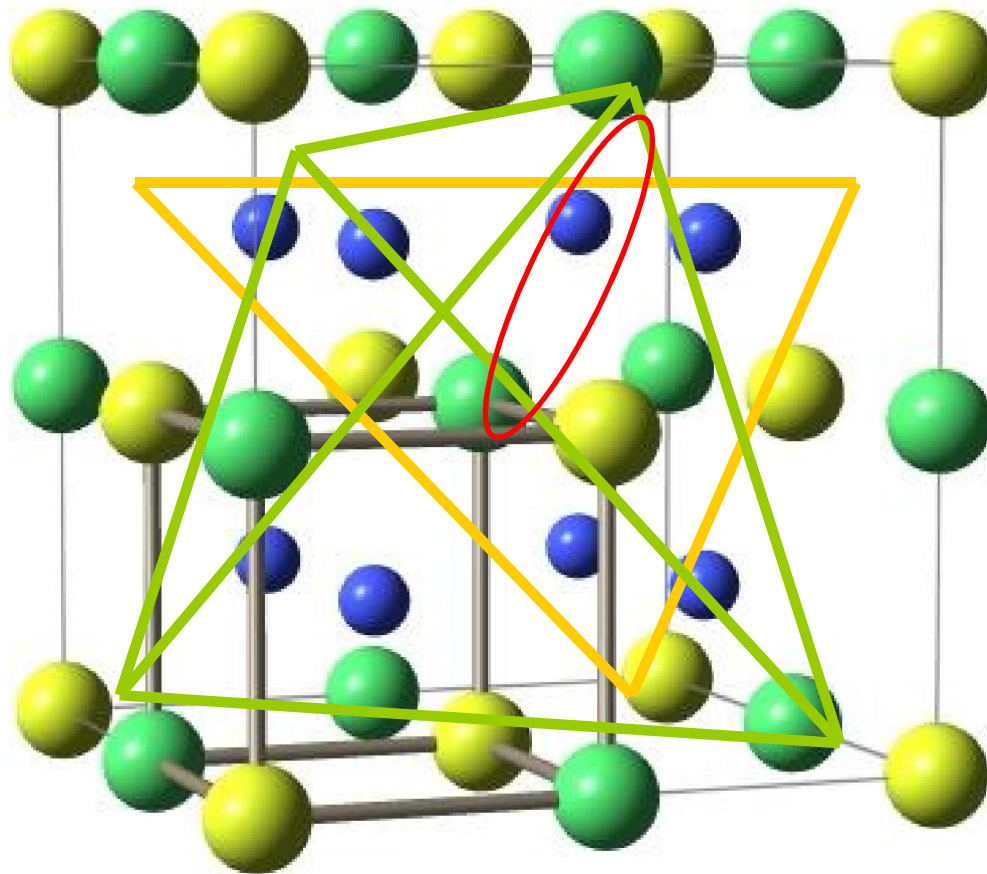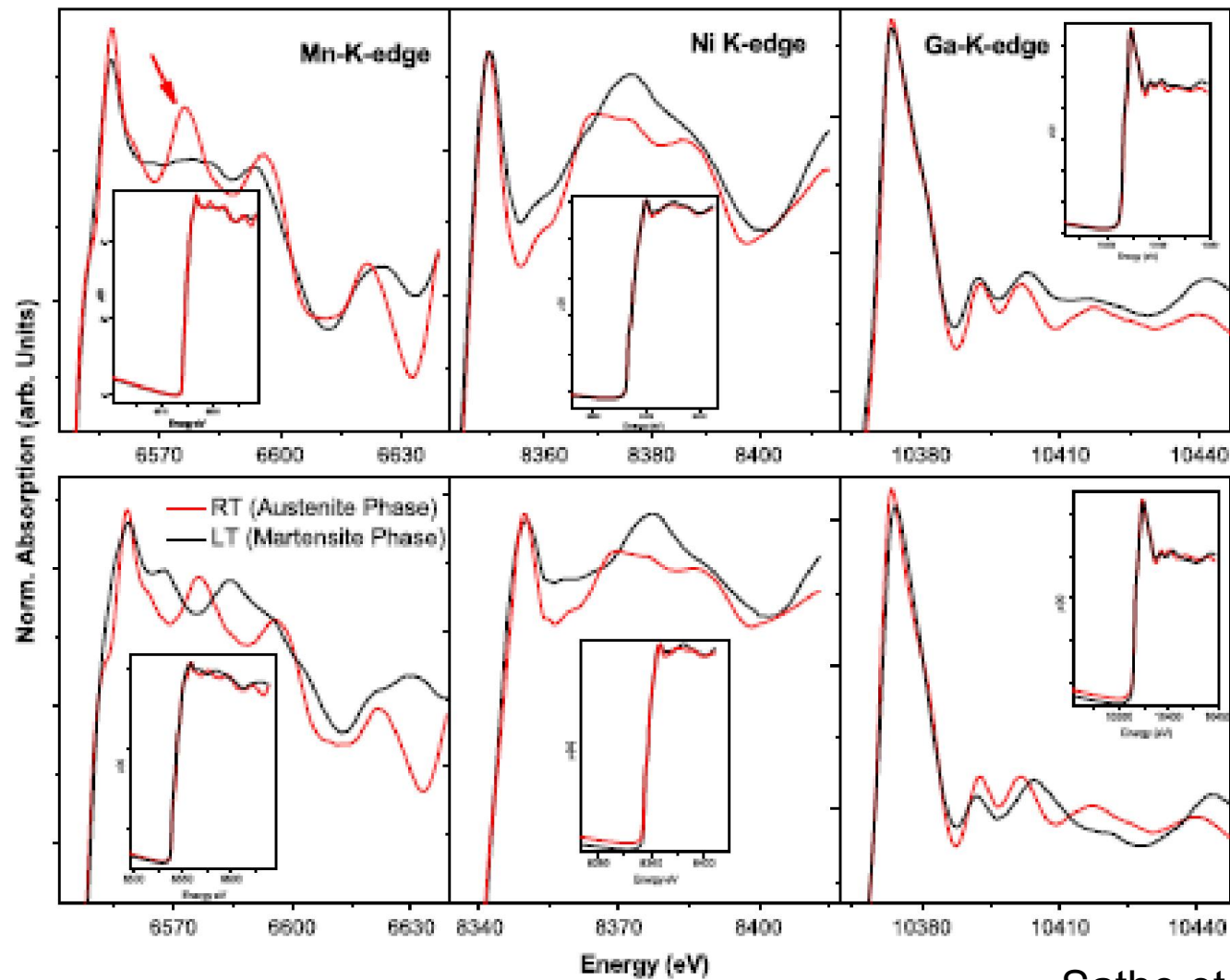
Summary of EXAFS Results

- Uneven movement of constituent atoms cause dimpling of planes giving rise to modulations.

- Mn has the largest amplitude of displacement while Ga atoms have the least.

- Upon martensitic transformation, Ga-Ni bond distance shorter than Mn-Ni.

- The effect is seen even in XANES features – indicates changes in hybridization – leads to re-distribution of electrons causing band Jahn-Teller effect.

HEXAGONAL MULTIFERROIC YMnO$_3$

- Hexagonal rare-earth (R) manganite RMnO3 has drawn much attention due to so-called multiferroicity with coexisting ferroelectricity and antiferromagnetism below 100 K.

- The correlation between otherwise, independent order parameters of polarization and magnetization is through a spin-lattice coupling.

- The ferroelectric polarization arises mainly from the R^{3+}-O^{2-} ionic displacements with relatively high transition temperatures.

- Possibility of manipulating the physical properties as well as the multiferroicity by controlling the physics at the Mn site.

Y(Mn,TM)O$_3$, TM = Co, Ni, Cu

Y(Mn,Zn)O$_3$

Zn–O   Zn K-edge EXAFS (a)

Zn–Cations $YMn_{0.9}Zn_{0.1}O_3$

Y–Cations   Y K-edge (b)
Y–O   EXAFS

$YMn_{0.9}Zn_{0.1}O_3$

$YMnO_3$

Mn–Cations   Mn K-edge (c)
Mn–O   EXAFS

$YMn_{0.9}Zn_{0.1}O_3$

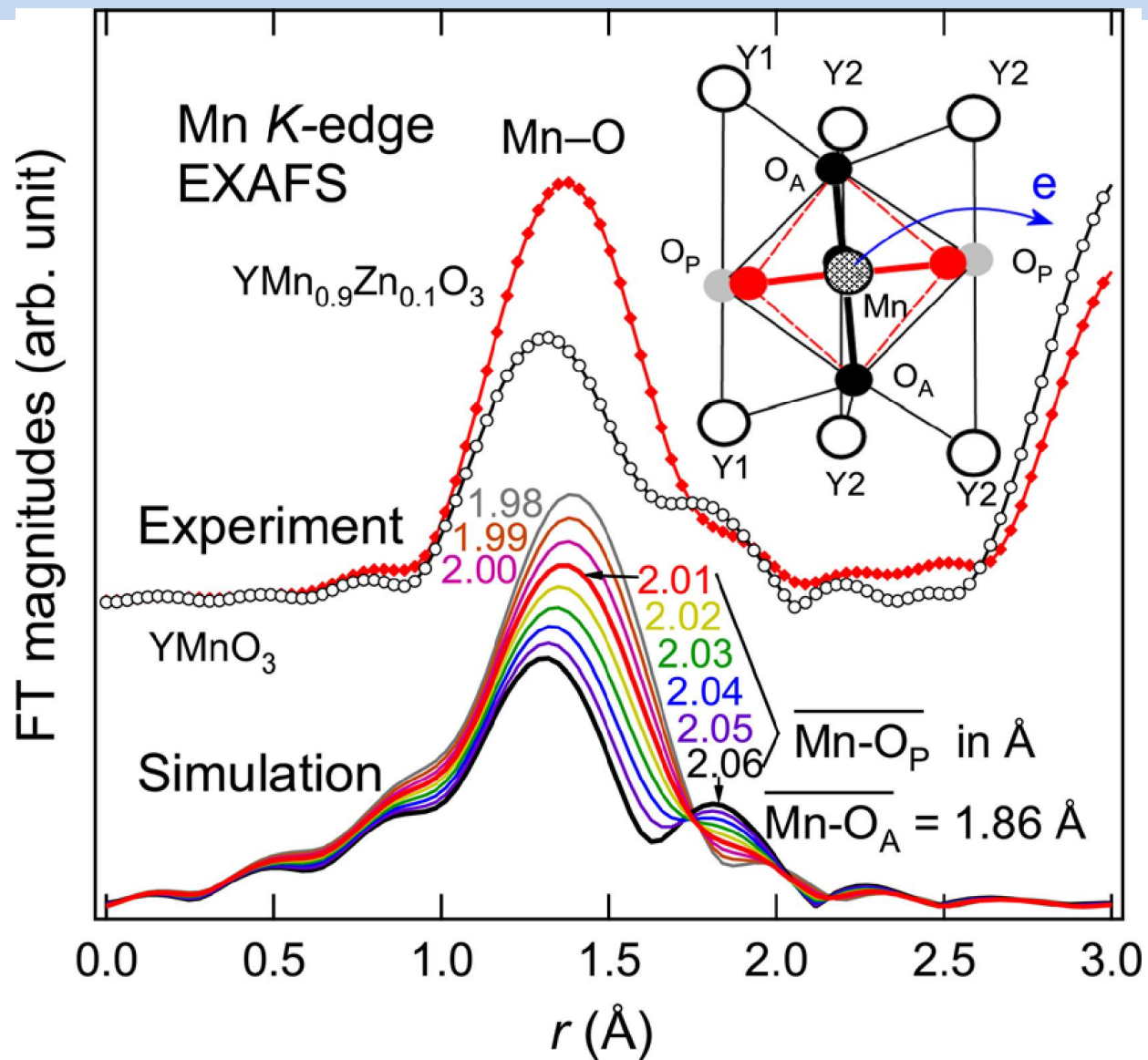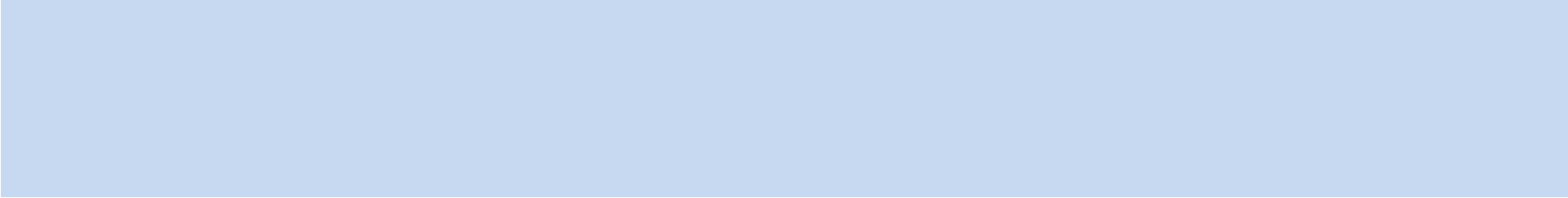$YMnO_3$

FT magnitudes (arb. units)

r (Å)
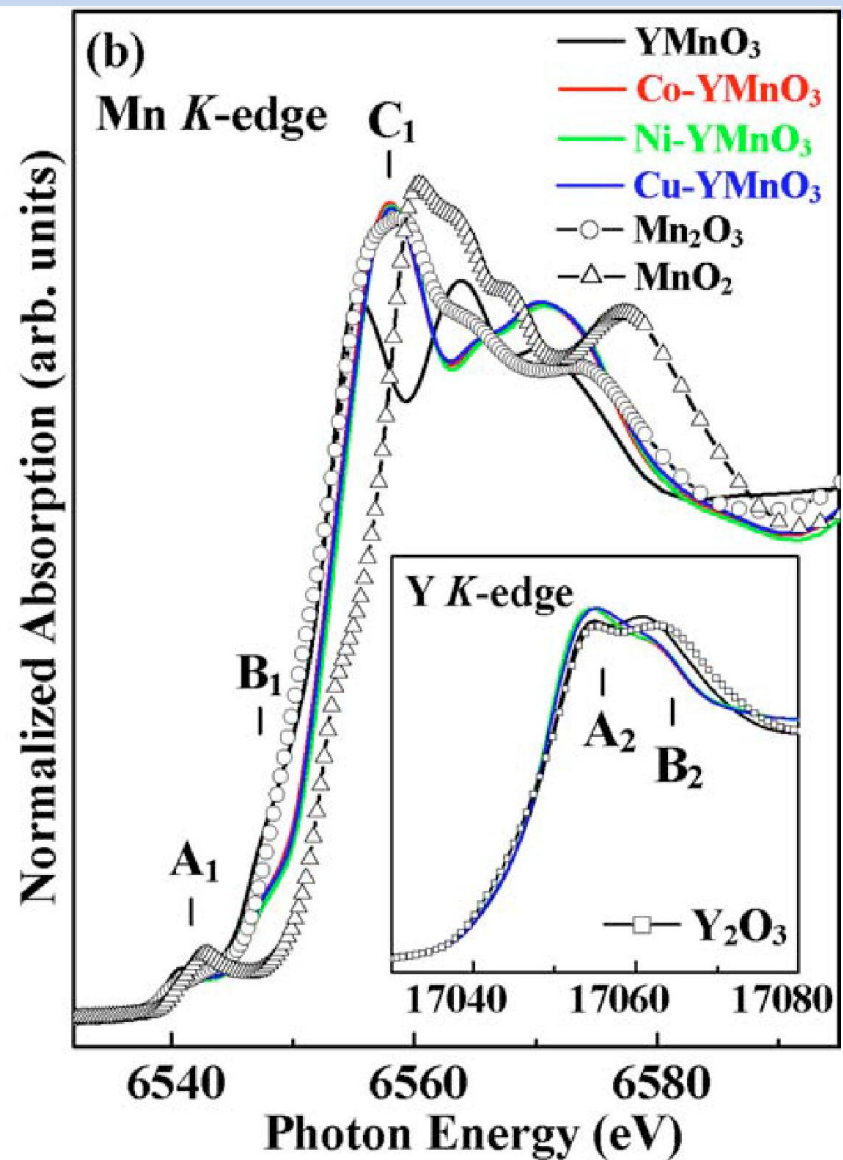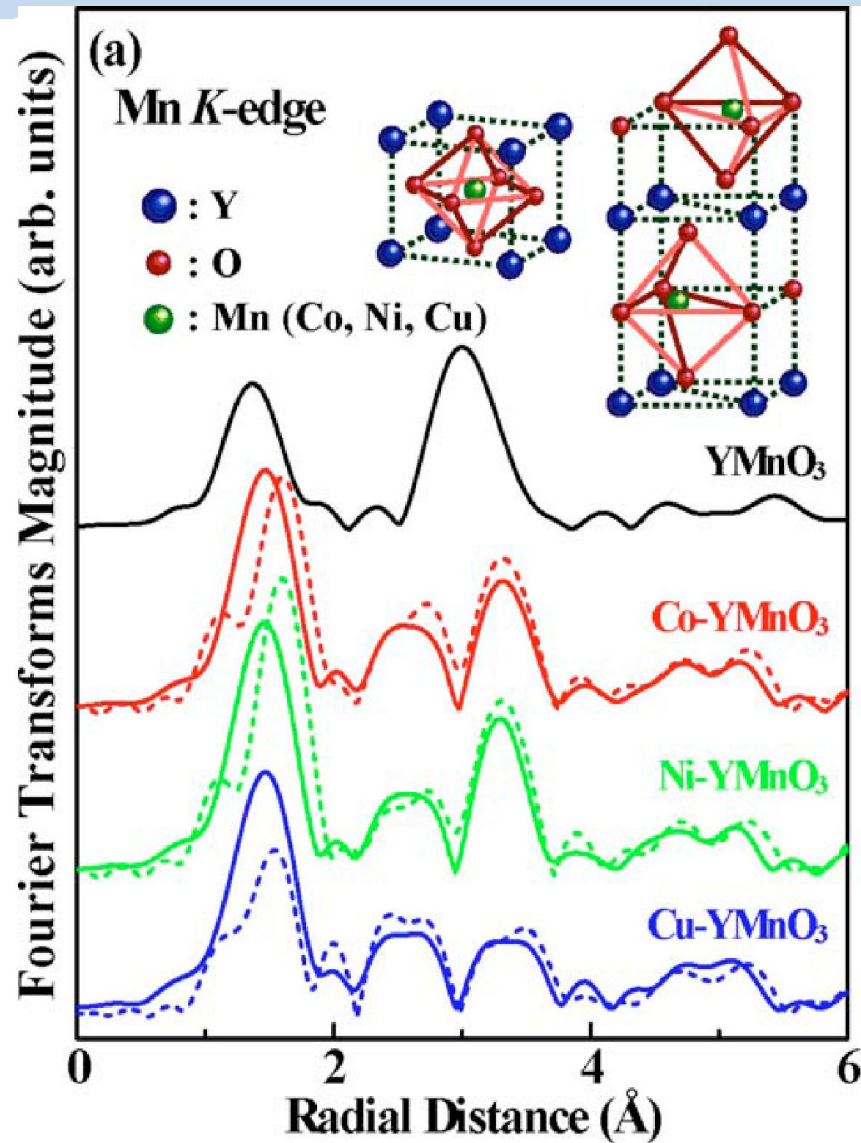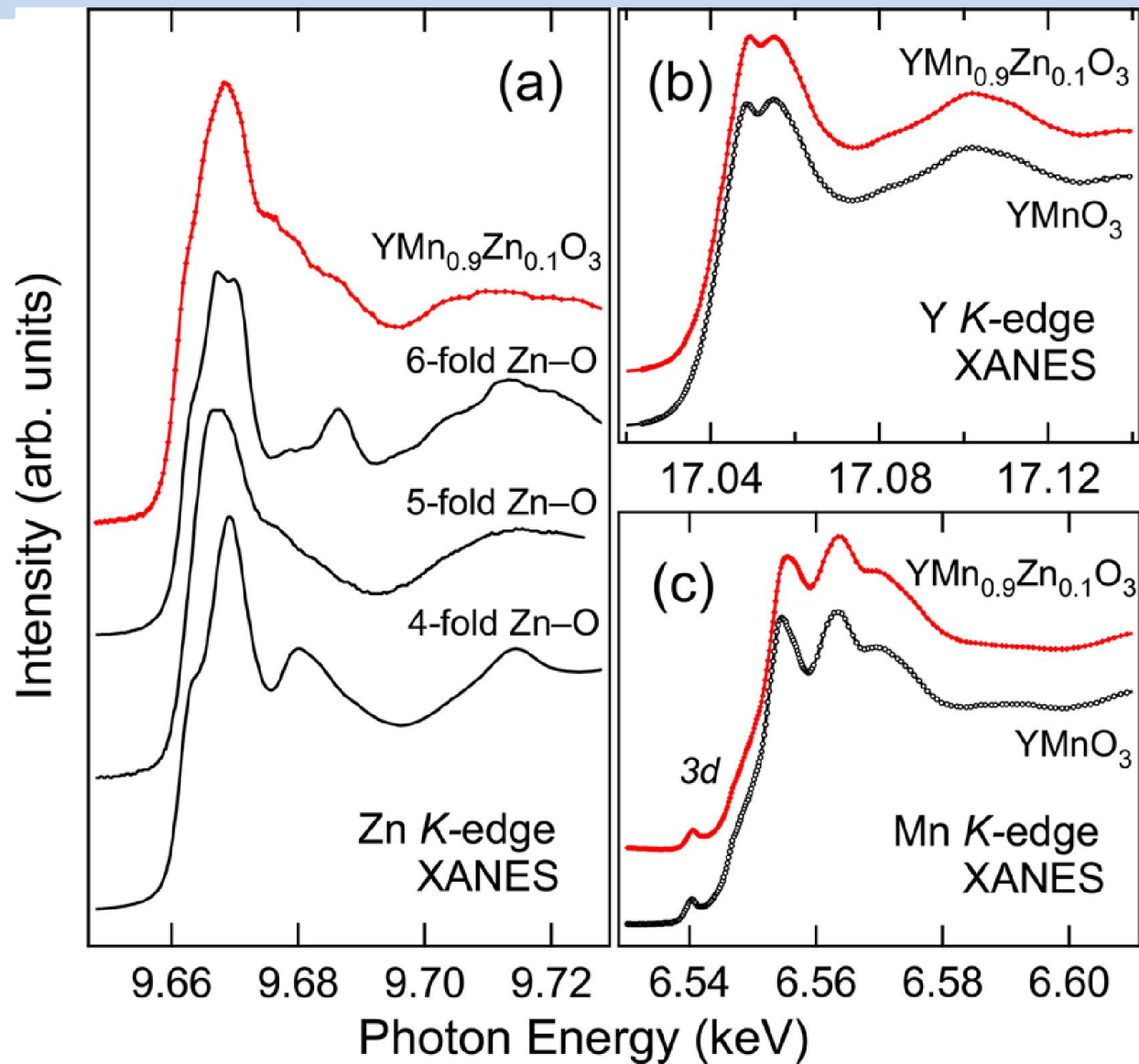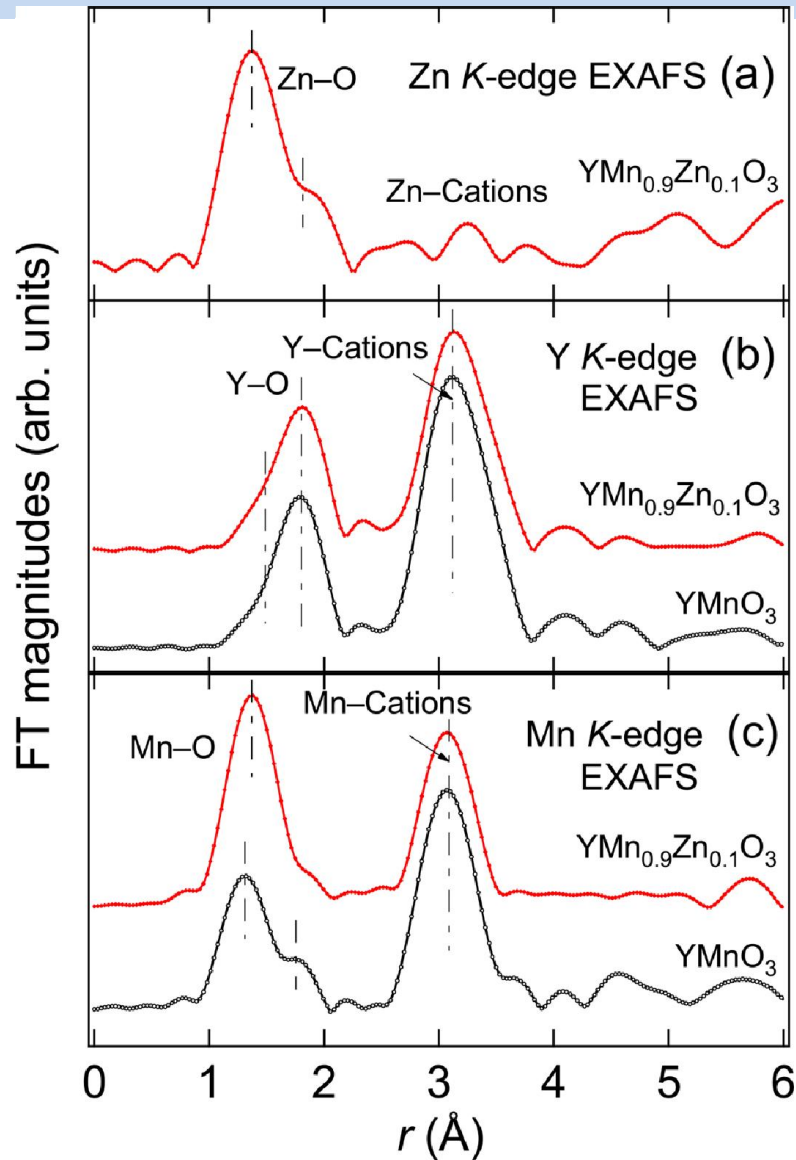
Two Zn – O bond distances

Y near neighbour environment not disturbed

Changes in Mn environment

GIANT MAGNETOCALORIC
$Gd_5(Ge_{1-x}Si_x)_4$ ALLOYS

- The family of giant magnetocaloric $Gd_5(Ge_{1-x}Si_x)_4$ materials continues to attract considerable attention due to its unusual magnetic properties and its potential for use in magnetic refrigeration near room temperature.

- The magnetostructural transformation involves displacement of Gd containing slabs along a directions destroying the Ge(Si) bonds along b direction.

- Breaking of these covalent bonds is believed to be responsible for destruction of FM order.
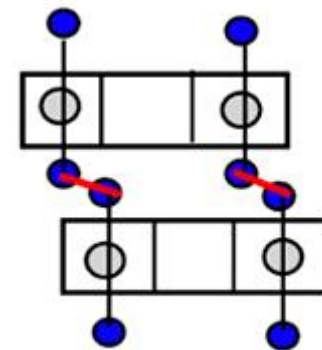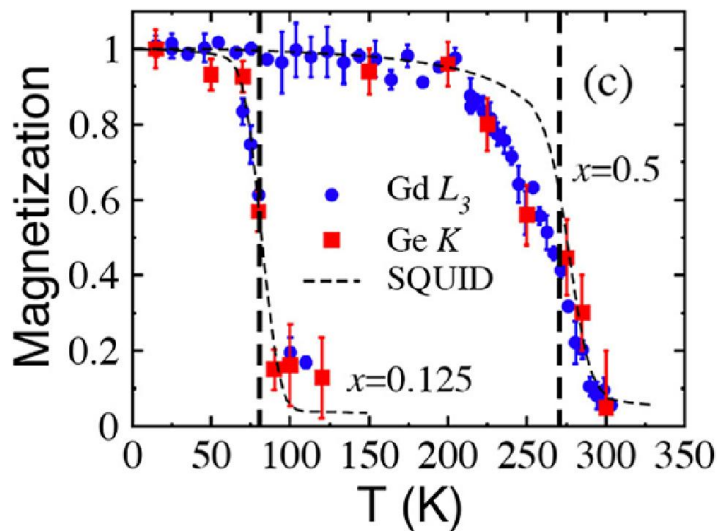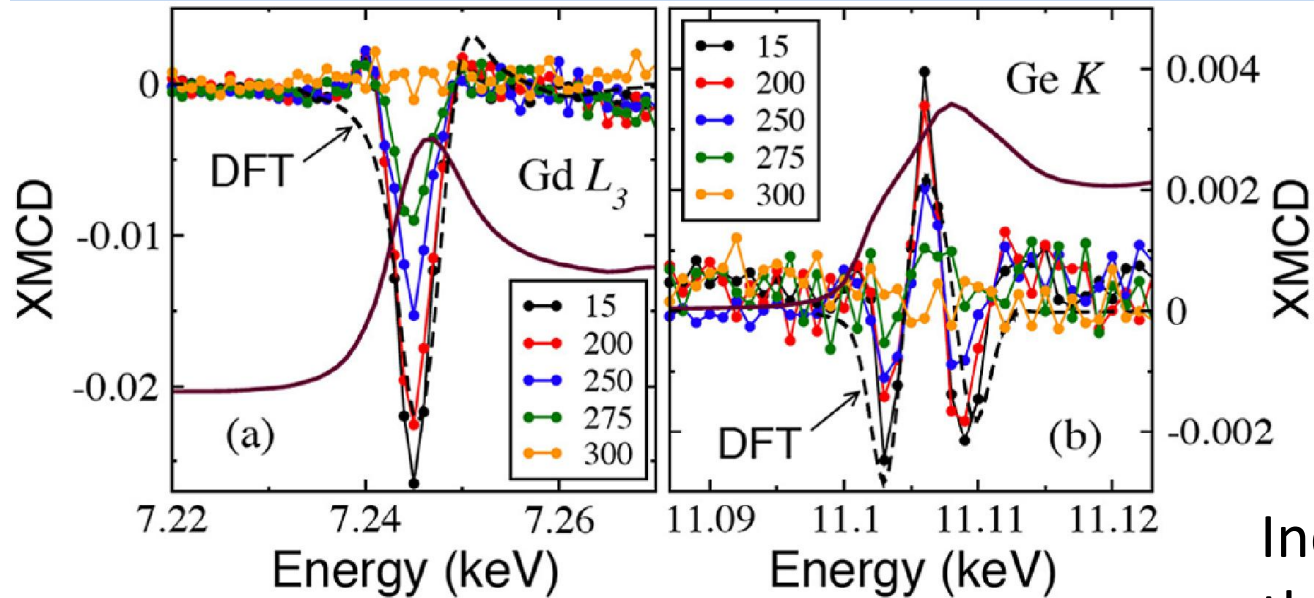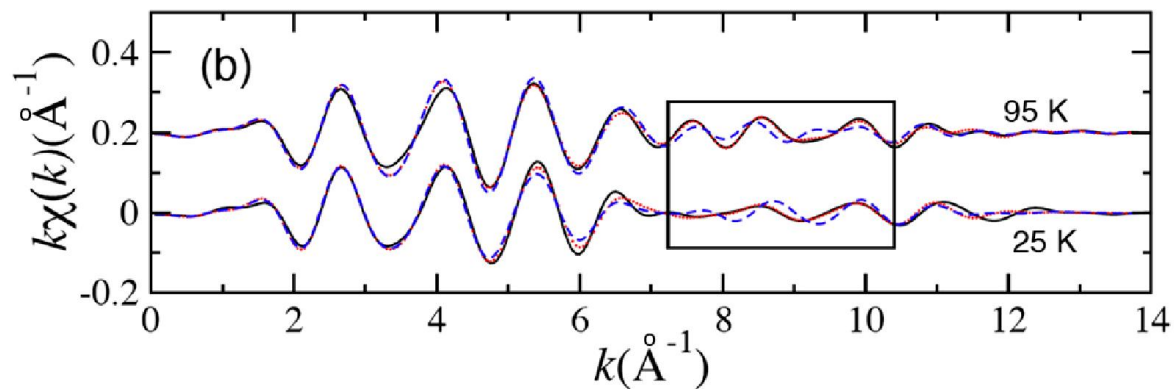
Induced moment on Ge through Gd(5d)-Ge(4p) hybridization.

The hybridization disappears at FM-PM transition.
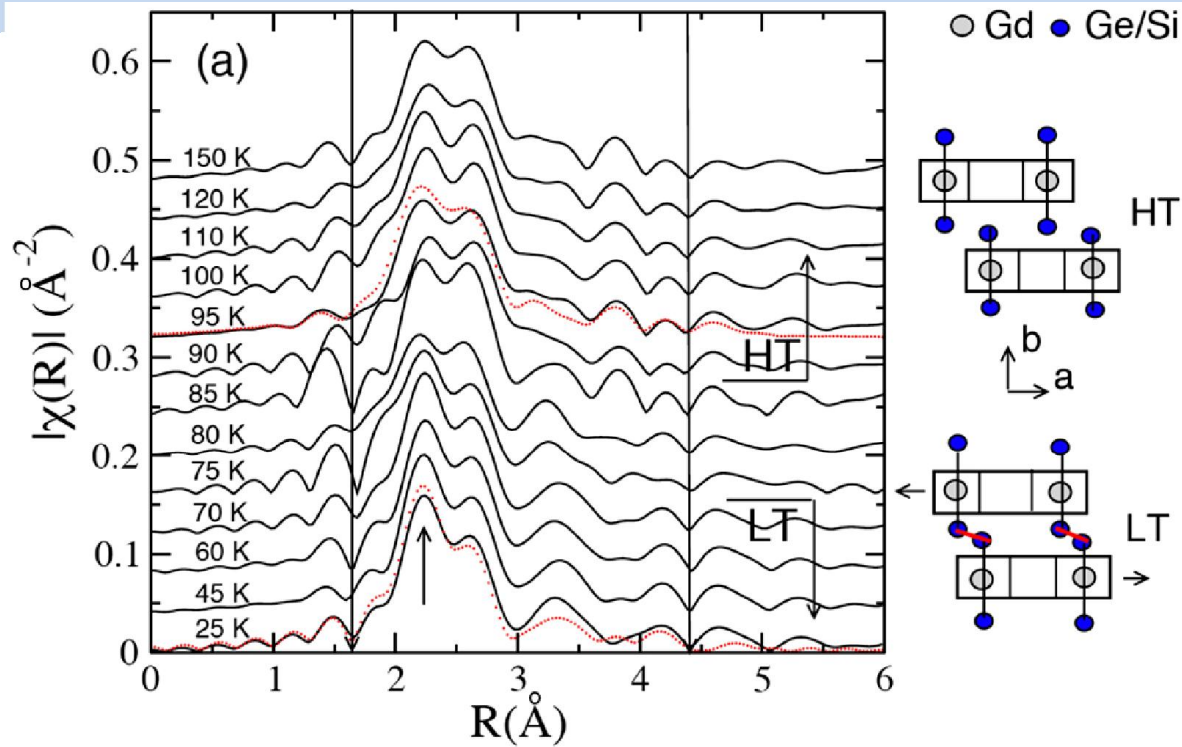
The slab-connecting Ge-Ge(Si) bonds change from a bonding distance of 2.67(1)Å to a nonbonding distance of 3.62(1) Å for $x = 0.125$.

- The spin-dependent hybridization between Ge $4p$ *and Gd 5d conduction states in* $Gd_5(Ge_{1-x}Si_x)_4$ alloys is modified by the bond-breaking magnetostructural transition reducing the net Gd $5d$ *moment and the strength* of FM RKKY exchange coupling across sheared slabs.

- The magnetic polarization at Ge sites is rooted in this hybridization and the agreement between XMCD experiment and theory validates our description of magnetization density, albeit only in the *O FM state.*
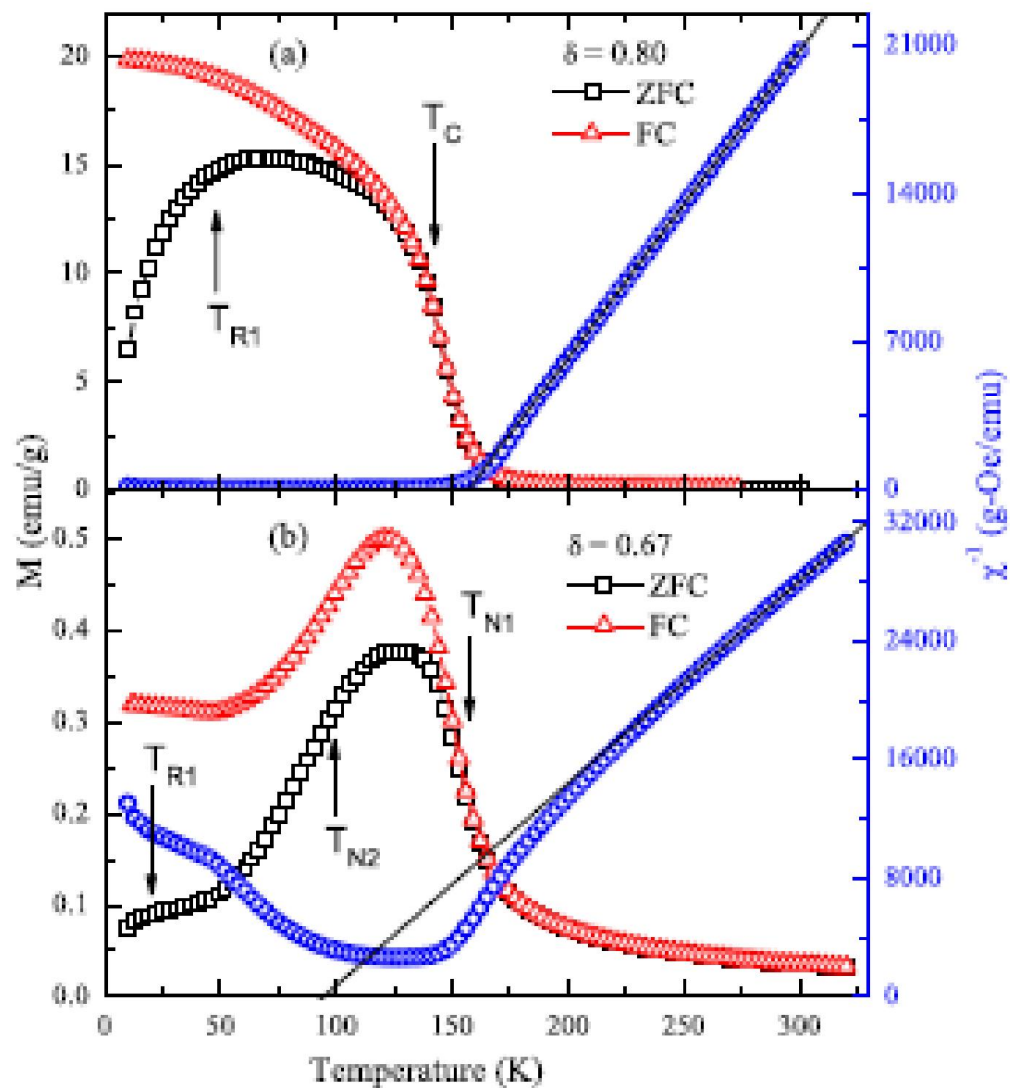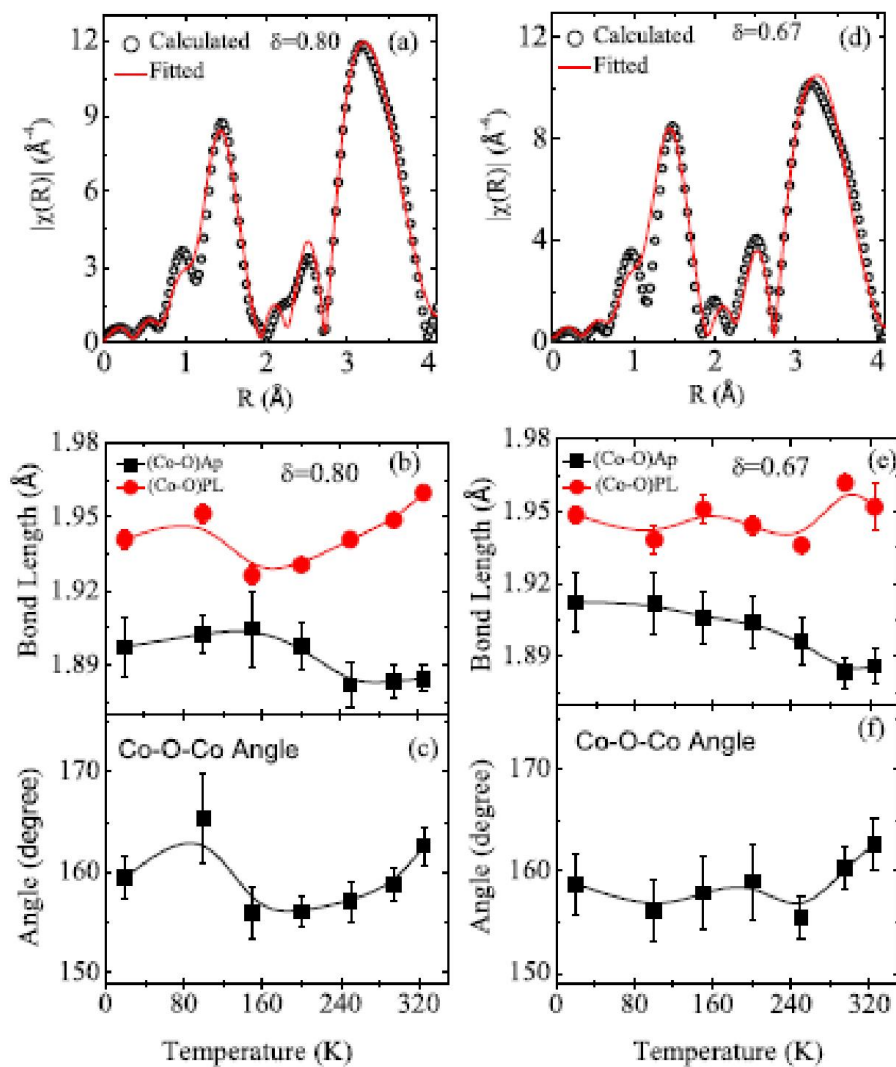
MAGNETIC PROPERTIES OF COBALTITES

PrBaCo$_2$O$_{5+\delta}$, $\delta > 0.5$
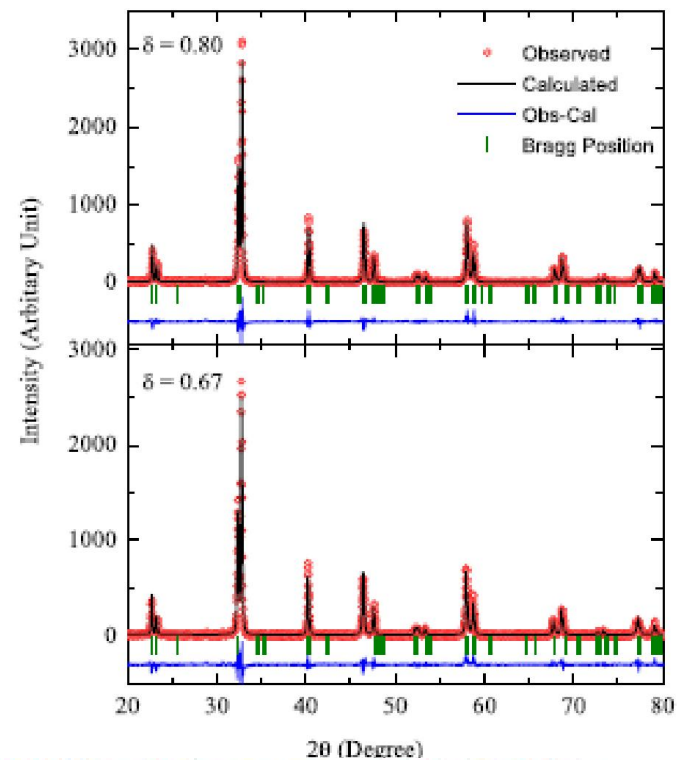
Table 1. Lattice parameters for PrBaCo$_2$O$_{5+\delta}$.

δ	a (Å)	b (Å)	c (Å)	V (Å^3)
0.80	3.9045(1)	3.9045(1)	7.6355(2)	116.410(7)
0.67	3.9085(7)	3.9085(7)	7.6311(2)	116.579(5)

EXAFS studies
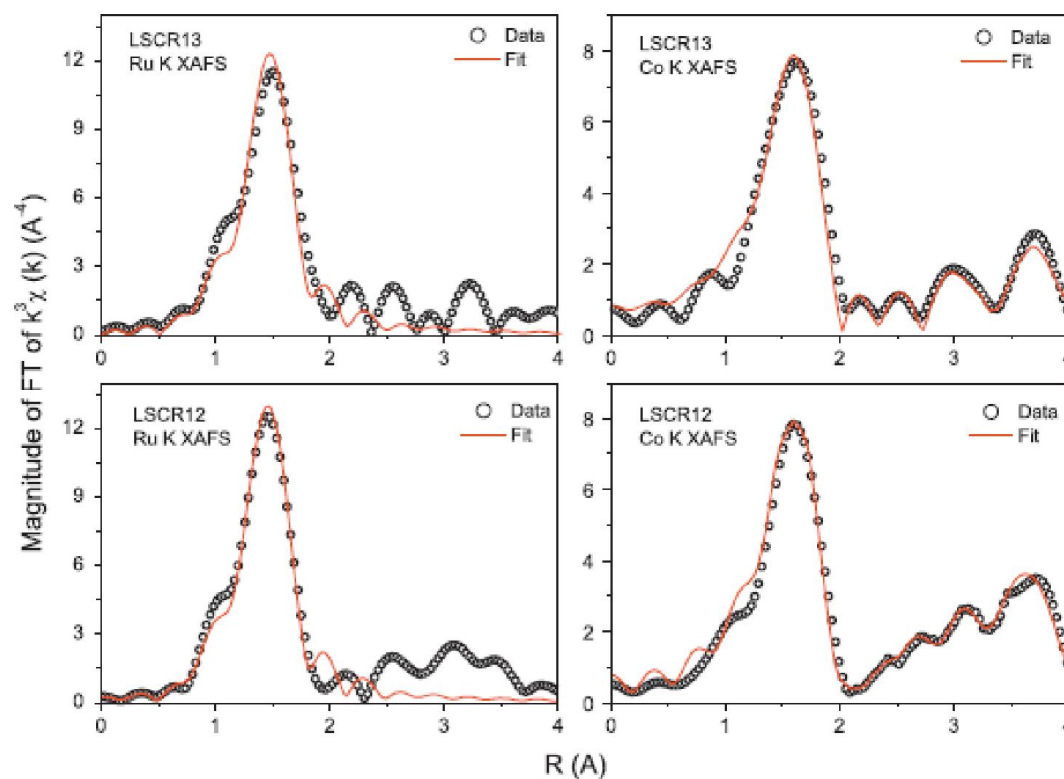

S. Ganorkar et al JPCM (2012)

LaSrCoRuO6 – effect of thermal disorder
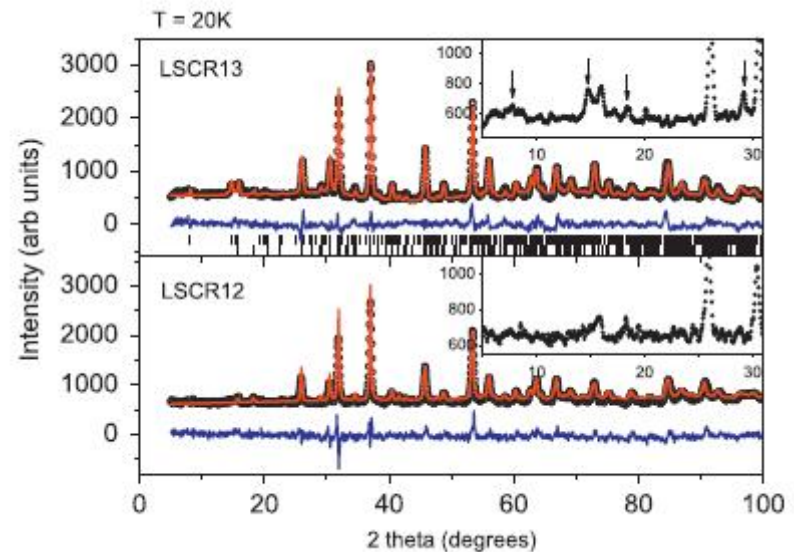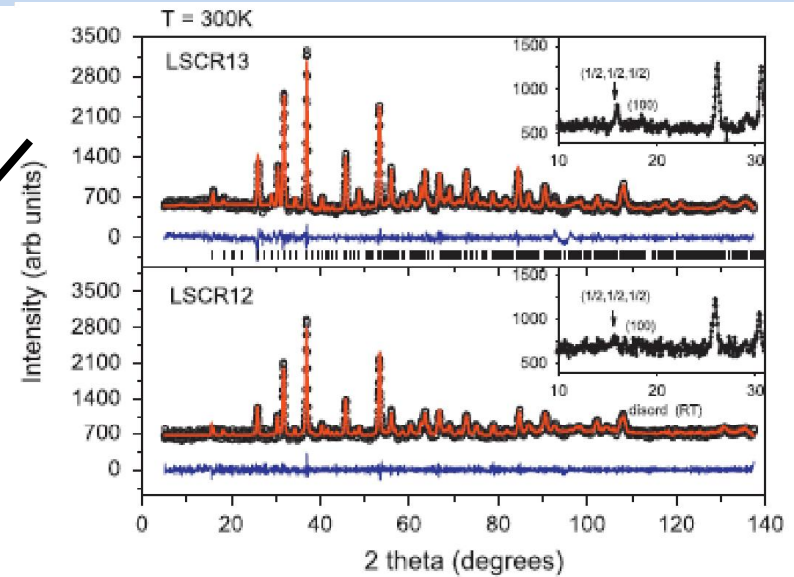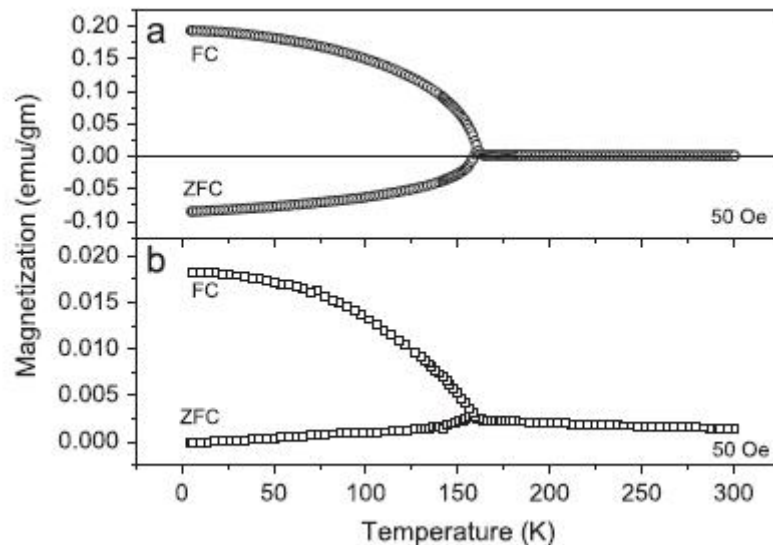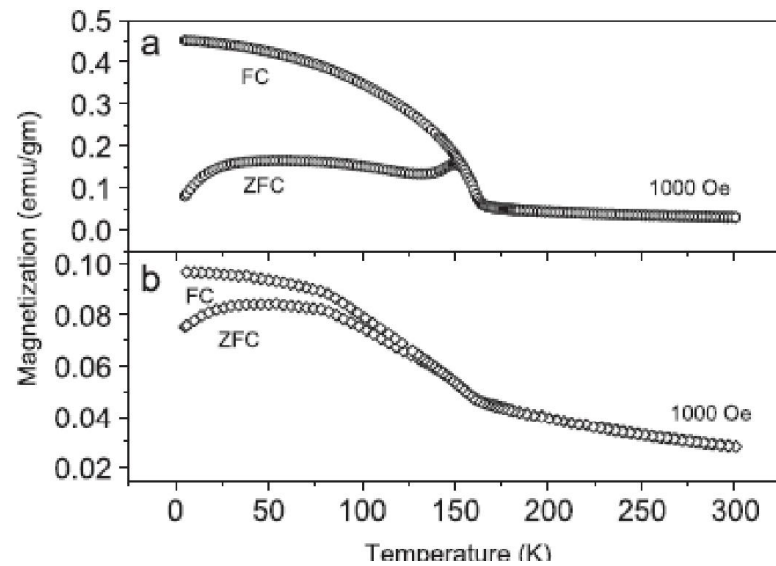
Co and Ru K EXAFS

Bond	LSCR 13		LSCR 12	
	R (Å)	σ^2 (Å^2)	R (Å)	σ^2 (Å^2)
Co–O	2.054(7)	0.008(1)	2.046(9)	0.009(1)
Ru–O	1.967(8)	0.003(1)	1.950(5)	0.004(1)
Co–Ru	3.97(6)	0.002(1)	3.97(1)	0.005(1)
Co–Ru–O–Co	4.00(7)	0.002(1)	4.00(1)	0.004(1)
∠ Co–O–Ru	161.7(1)°		166.4(1)°	

P. S. R. Murthy et al JMMM 322 (2010)

Thank you